Title

Discovery of several thousand highly diverse circular DNA viruses

Authors

Michael J. Tisza[1], Diana V. Pastrana[1], Nicole L. Welch[1], Brittany Stewart[1], Alberto Peretti[1], Gabriel J. Starrett[1], Yuk-Ying S. Pang[1], Siddharth R. Krishnamurthy[2], Patricia A. Pesavento[3], David H. McDermott[4], Philip M. Murphy[4], Jessica L. Whited [5,6,7], Bess Miller [5,6], Jason M. Brenchley[8], Stephan P. Rosshart[9], Barbara Rehermann[9], John Doorbar[10], Blake A. Ta'ala[11], Olga Pletnikova[12], Juan Troncoso[12], Susan M. Resnick[13], Ben Bolduc[14], Matthew B. Sullivan[14,15], Arvind Varsani[16,17], Anca M. Segall[18], Christopher B. Buck[1,19]*

Affiliations

[1]Lab of Cellular Oncology, NCI, NIH, Bethesda, MD 20892-4263
[2]Metaorganism Immunity Section, Laboratory of Immune System Biology, NIAID, NIH, Bethesda, MD 20892-4263
[3]Department of Pathology, Microbiology, and Immunology, University of California, Davis, CA 95616, USA.
[4]Molecular Signaling Section, Laboratory of Molecular Immunology, NIAID, Bethesda, Maryland, USA.
[5]Department of Orthopedic Surgery, Harvard Medical School, The Harvard Stem Cell Institute, Brigham and Women's Hospital, 60 Fenwood Road, Boston, MA, 02115, USA.
[6]Broad Institute of MIT and Harvard, 7 Cambridge Center, Cambridge, MA, 02142, USA.
[7]Department of Stem Cell and Regenerative Biology, Harvard University, 7 Divinity Avenue, Cambridge, MA, 02138, USA.
[8]Barrier Immunity Section, Lab of Viral Diseases, NIAID, NIH, MD 20892
[9]Immunology Section, Liver Diseases Branch, NIDDK, NIH, Bethesda, MD 20892-1800
[10]Department of Pathology, University of Cambridge, Tennis Court Road, Cambridge, CB2 1QP, UK.
[11]Mililani Mauka Elementary, Mililani, HI, 96789, USA.
[12]Department of Pathology (Neuropathology), Johns Hopkins University School of Medicine, Baltimore, MD, USA.
[13]Laboratory of Behavioral Neuroscience, National Institute on Aging, Baltimore, MD 21224, USA.
[14]Department of Microbiology, Ohio State University, Columbus, Ohio, United States
[15]Civil, Environmental and Geodetic Engineering, Ohio State University, Columbus, Ohio, United States
[16]The Biodesign Center of Fundamental and Applied Microbiomics, School of Life Sciences, Center for Evolution and Medicine, Arizona State University, 1001 S. McAllister Ave, Tempe, AZ 85287-5001, USA
[17]Structural Biology Research Unit, Department of Clinical Laboratory Sciences, University of Cape Town, Rondebosch, 7701, Cape Town, South Africa.
[18]Viral Information Institute & Department of Biology, San Diego State University, San Diego, CA, 92182-4614, USA.
[19]Lead contact
*Correspondence: buckc@mail.nih.gov

Summary

Although it is suspected that there are millions of distinct viral species, fewer than 9,000 are catalogued in GenBank's RefSeq database. We selectively enriched for and amplified the genomes of circular DNA viruses in over 70 animal samples, ranging from cultured soil nematodes to human tissue specimens. A bioinformatics pipeline, Cenote-Taker, was developed to automatically annotate over 2,500 circular genomes in a GenBank-compliant format. The new genomes belong to dozens of established and emerging viral families. Some appear to be the result of previously undescribed recombination events

between ssDNA viruses and ssRNA viruses. In addition, hundreds of circular DNA elements that do not encode any discernable similarities to previously characterized sequences were identified. To characterize these "dark matter" sequences, we used an artificial neural network to identify candidate viral capsid proteins, several of which formed virus-like particles when expressed in culture. These data further the understanding of viral sequence diversity and allow for high throughput documentation of the virosphere.

Keywords
Viral metagenomics, virome, virus discovery, microbial genomics, evolution

Introduction

There has been a rush to utilize the massive parallel sequencing approaches to better understand the complex microbial communities associated with humans and other animals. Although the bacterial populations in these surveys have become increasingly recognizable (Lloyd-Price et al., 2017), a substantial fraction of the reads and *de novo* assembled contigs in many metagenomics efforts are binned as genetic "dark matter," with no recognizable similarity to characterized sequences (Krishnamurthy and Wang, 2017, Oh et al., 2014). Some of this dark matter undoubtedly consists of viral sequences, which have remained poorly characterized due to their enormous diversity (Simmonds et al., 2017, Paez-Espino et al., 2016, Emerson et al., 2018). Recent efforts have shown that our understanding of viral diversity, even of viruses known to directly infect humans, has been incomplete (Pastrana et al., 2018, Turnbaugh et al., 2007, Gilbert et al., 2010). To increase the power of future studies seeking to more comprehensively catalog the virome and find additional associations between viruses and disease, reference genomes for all clades of the virosphere need be identified, annotated, and made publicly accessible.

Virus discovery has typically proven to be more difficult than discovery of cellular organisms. Whereas all known cellular organisms encode conserved sequences (such as ribosomal RNA genes) that can readily be identified through sequence analysis, viruses, as a whole, do not have any universally conserved sequence components (O'Leary et al., 2016, Brister et al., 2015, Sullivan, 2015, Rohwer and Edwards, 2002). Nevertheless, some success has been achieved in RNA virus discovery by probing for the conserved sequences of their distinctive RNA-dependent RNA polymerase or reverse transcriptase genes in metatranscriptomic data (Shi et al., 2016). Also, many bacteriophages of the order *Caudovirales*, such as the families *Siphoviridae*, *Podoviridae*, and *Myoviridae*, have been reported in high numbers due to their and their hosts' culturability and their detectability using viral plaque assays (Pope et al., 2015, Grose and Casjens, 2014, Grose et al., 2014). The relatively abundant representation of these families in databases has allowed new variants to be recognized by high-throughput virus classification tools like VirSorter (Roux et al., 2015, Gregory et al., 2019, Roux et al., 2019b). In contrast, many small DNA viruses are not easily cultured (Bedell et al., 1991), use diverse genome replication strategies, and typically lack DNA polymerase genes such as those in large DNA viruses (Koonin et al., 2015). An additional challenge is that small DNA viruses with segmented genomes may have segments that do not encode recognizable homologs of known viral genes. Therefore, small DNA viruses are more sparsely represented in reference databases. However, some groups have been successful in discovery of small DNA genomes in a wide range of viromes (Blinkova et al., 2010, Pastrana et al., 2018, Dayaram et al., 2015, Dayaram et al., 2016, Labonte and Suttle, 2013, Rosario et al., 2018, Victoria et al., 2009).

Despite the apparent challenges in detecting small DNA viruses, many have physical properties that can be leveraged to facilitate their discovery. In contrast to the nuclear genomes of animals, many DNA virus genomes have circular topology, which allows selective enrichment through rolling circle amplification (RCA) methods (Kim et al., 2008). Further, the unique ability of viral capsids to protect

96 nucleic acids from nuclease digestion and to mediate the migration of the viral genome through
97 ultracentrifugation gradients or size exclusion columns allows physical isolation of viral genomes.
98 The current study grew out of an effort to find papillomaviruses (small circular DNA viruses) in
99 humans and economically important or evolutionarily informative animals (Pastrana et al., 2018, Peretti
100 et al., 2015). The sampling included several types of animals that might serve as laboratory models (e.g.,
101 mice, fruit flies, soil nematodes). A number of papillomaviruses were detected among a vastly larger set
102 of circular DNA sequences that were not easily identifiable in standard BLASTN searches. The goal of the
103 present study is to catalog and annotate the circular DNA virome from these animal tissues to
104 understand the diversity and evolution of viral sequences. We developed a comprehensive
105 bioinformatics pipeline, Cenote-Taker, to classify and annotate over 2,500 candidate viral genomes and
106 generate GenBank-compliant output files. Cenote-Taker is available for free public use with a graphical
107 user interface at http://www.cyverse.org/discovery-environment.
108
109 **Results**
110 **Virion enrichment, genome sequencing, and annotation**
111 We have previously developed methods for discovery of new polyomavirus and papillomavirus species
112 in skin swabs and complex tissue specimens (Peretti et al., 2015). Nuclease-resistant DNA from purified
113 virions was amplified by random-primed rolling circle amplification (RCA) and subjected to deep-
114 sequencing. Reads were *de novo* assembled into contigs and analyzed with a bioinformatics pipeline,
115 Cenote-Taker (a portmanteau of *cenote*, a naturally occurring circular water pool, and *note-taker*), to
116 identify and annotate *de novo* assembled contigs with terminal direct repeats consistent with circular
117 DNA molecules. In this pipeline, putative circular sequences were queried against GenBank's nucleotide
118 database using BLASTN to remove circles with extensive nucleotide identity (>90% across any 500 bp
119 window) to known sequences. Sequences with >90% identity to previously reported viral sequences
120 represented less than 1.5% of circular contigs and are not included in further analysis. Open reading
121 frames (ORFs) from remaining unidentified circular DNA sequences >240 nucleotides (nt) in length were
122 translated and used for RPS-BLAST queries of GenBank's Conserved Domain Database (CDD). ORFs that
123 did not yield E values better than 1×10^{-4} in RPS-BLAST were subjected to BLASTP searches of viral
124 sequences in GenBank's nr database (Altschul et al., 1990, Marchler-Bauer and Bryant, 2004, Marchler-
125 Bauer et al., 2015). For ORFs that were not confidently identified in BLAST searches, HHBlits (Remmert
126 et al., 2011) was used to search the CDD, Pfam (El-Gebali et al., 2019), Uniprot (UniProt, 2019), Scop
127 (Chandonia et al., 2019), and PDB (Burley et al., 2017) databases. The results were used to annotate and
128 name each sequence in a human-readable genome map as well as a format suitable for submission to
129 GenBank. After checking the Cenote-Taker output of each genome, minor revisions were made, as
130 needed, and files were submitted to GenBank (BioProject Accessions PRJNA393166 and PRJNA396064).
131 All annotations meet or exceed recently proposed standards for uncultivated virus genomes (Roux et al.,
132 2019a).
133
134 **Discovery of 2514 DNA viruses in animal metagenomes**
135 Of the novel circular sequences detected in the survey, 1844 encode genes with similarity to proteins of
136 ssDNA viruses and 55 encode genes with similarity to dsDNA viral proteins (Fig. 1A). The large majority
137 of genomes from this study are highly divergent from RefSeq entries (Fig. S1). We discovered 868
138 genomes that had similarity to unclassified eukaryotic viruses known as circular replication associated
139 protein (Rep)-encoding single-stranded DNA (CRESS) viruses. The group is defined by the presence of a
140 characteristic rolling circle endonuclease/superfamily 3 helicase gene (Rep) (Zhao et al., 2019,
141 Kazlauskas et al., 2019), but has not been assigned to families by the ICTV or RefSeq. We estimate that
142 199 non-redundant unclassified CRESS virus genomes had been previously deposited in GenBank, and 85
143 are listed in RefSeq (Fig. 1B). Also abundant was the viral family *Microviridae*, a class of small

Figure 1: Novel viruses associated with animal samples

Gross characterization of viruses discovered in this project compared to NCBI RefSeq virus database entries. (A) Pie chart representing the number of viral genomes in broad categories. (B) Bar graph showing the number of new representatives of known viral families or unclassified groups. Note that genomes in this study were assigned taxonomy based on at least one region with a BLASTX hit with an E value <1×10-5, suggesting commonality with a known viral family. Some genomes may ultimately be characterized as being basal to the assigned family.

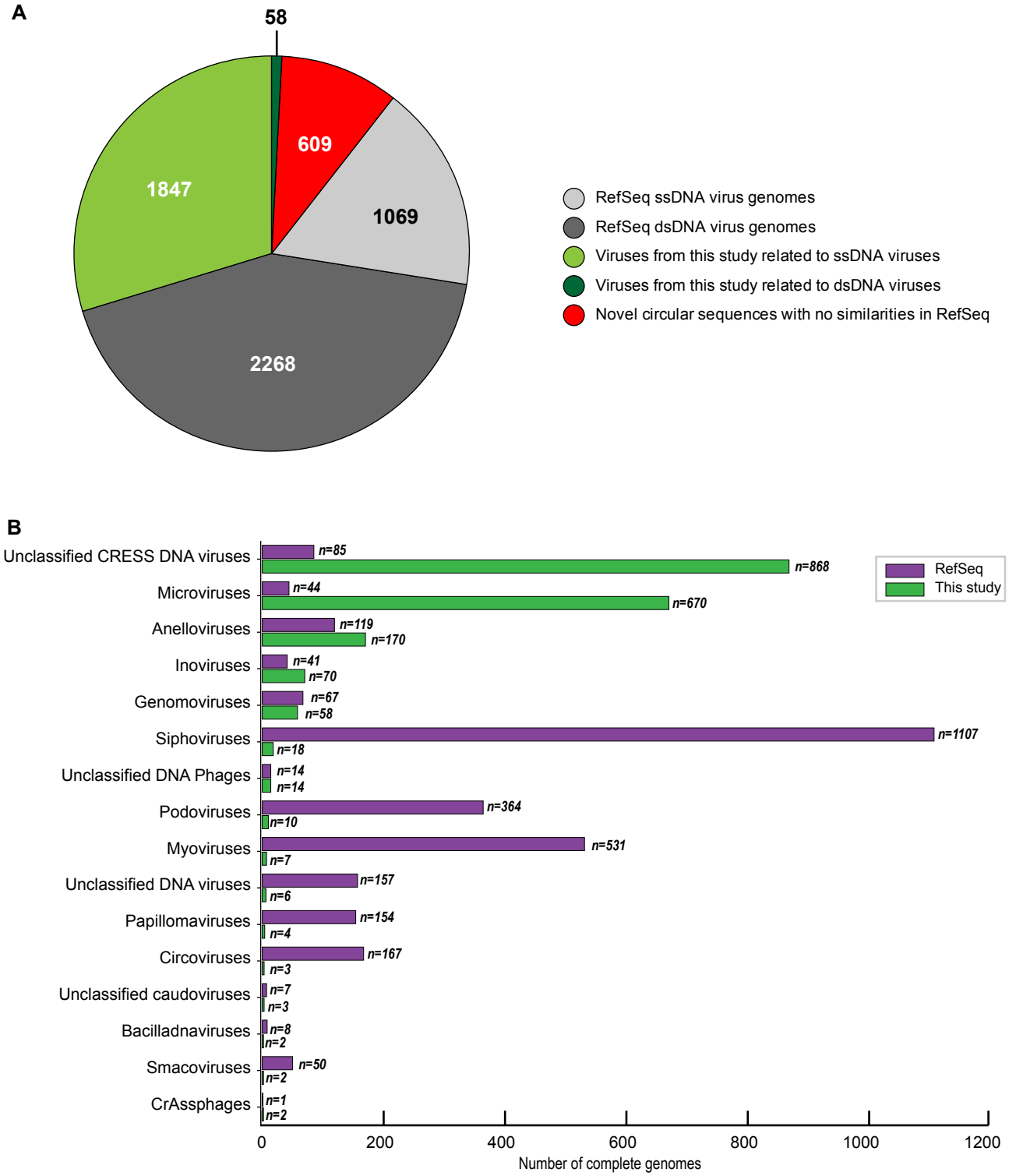

Supplemental Figure 1: Divergence of proteins encoded by circular contigs

BLASTX summary of each circular DNA molecule recovered from virus enriched samples. Sequences were queried against a database of viral and plasmid sequences. Only hits with E values < 10-5 were plotted. Here, BLASTX only reports the most significant stretch of amino acid sequence from each circular contig, and, therefore, other regions of each contig can be assumed to be equally or less conserved.

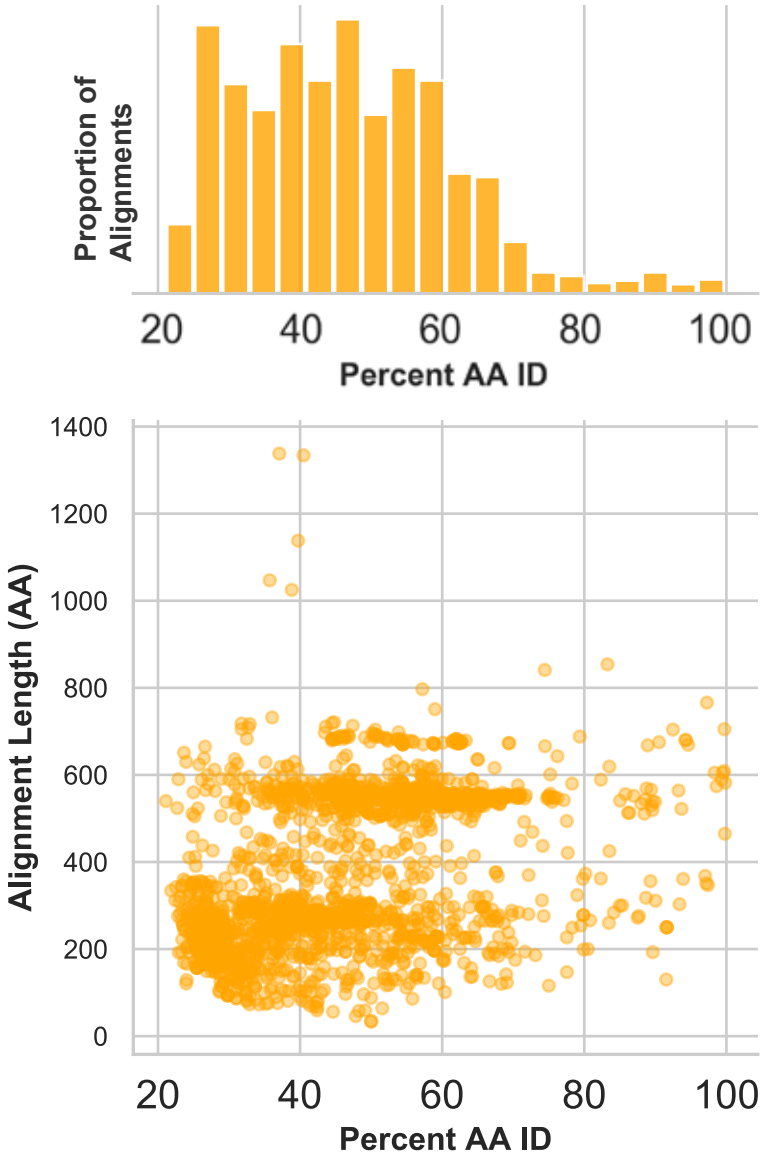

144 bacteriophages, with 670 complete genomes. This represents a substantial expansion beyond the 459
145 non-redundant microvirus genomes previously listed in GenBank (of which 44 were listed in the RefSeq
146 database). Other genomes that were uncovered represent *Anelloviridae* (n=170), *Inoviridae* (n=70),
147 *Genomoviridae* (n=58), *Siphoviridae* (n=18), unclassified phage (n=14), *Podoviridae* (n=10), *Myoviridae*
148 (n=7) unclassified virus (n=6), *Papillomaviridae* (n=4), *Circoviridae* (n=3), unclassified *Caudovirales* (n=3),
149 *Bacilladnaviridae* (n=2), *Smacoviridae* (n=2), and *CrAssphage* (n=2) (Fig. 1B).
150 It is difficult to assign a host to most of the viruses from this study due to their divergence from
151 known viral sequences. However, we searched the CRISPR database at (https://crispr.i2bc.paris-
152 saclay.fr/crispr/BLAST/CRISPRsBlast.php), and three viruses had exact matches to CRISPR spacers in
153 bacterial genomes (Siphoviridae sp. ctcj11:Shewanella sp. W3-18-1, Inoviridae sp. ctce6:Shewanella
154 baltica OS195, Microviridae sp. ctbe523:Paludibacter propionicigenes WB4) and one virus had an exact
155 match to the CRISPR spacer of an archaeon (Caudovirales sp. cthg227:Methanobrevibacter sp. AbM4),
156 implying that these organisms are infected by these viruses. Further, the 142 anelloviruses found in
157 human blood samples (Table S1) are almost certain to be bona fide human viruses based on their
158 relatedness to known human anelloviruses.
159 In addition to circular genomes with recognizable similarity to known viruses, 609 circular
160 contigs appeared to represent elements that lacked discernable similarity to known viruses (Fig. 1A).
161 The vast majority of the *de novo* assembled circular genomes were <10 kb in length (Fig S2). This
162 is largely due to the fact that large genomes are typically more difficult to *de novo* assemble from short
163 reads. Despite these technical obstacles, our detection of a new tailed bacteriophage with a 419kb
164 genome (Myoviridae sp. isolate ctbc_4, GenBank Accession: MH622943), along with 45 other >10 kb
165 circular sequences (Fig S2), indicates that the methods used for the current work can detect large viral
166 genomes.
167 There has been a recent renewal of interest in the hypothesis that viruses may be etiologically
168 associated with degenerative brain diseases, such as Alzheimer's disease (Itzhaki et al., 2016, Eimer et
169 al., 2018). Conflicting literature suggests the possible presence of papillomaviruses in human brain tissue
170 (Coras et al., 2015, Chen et al., 2012). Samples of brain tissue from individuals who died of Alzheimer's
171 disease (n=6) and other forms of dementia (n=6) were subjected to virion enrichment and deep
172 sequencing. Although complete or partial genomes of known papillomaviruses, Merkel cell
173 polyomavirus, and/or anelloviruses were observed in some samples (Supplementary File S1), no novel
174 complete viral genomes were recovered (Table S1). No viral sequences were detected in a follow-up
175 RNA deep sequencing analysis of the brain samples. It is difficult to know how to interpret these
176 negative data. It is conceivable that the known viral DNA sequences observed in the Optiprep-RCA
177 samples represent virions from blood vessels or environmental sources.
178 It has recently become apparent that certain nucleic acid extraction reagents are contaminated
179 with viral nucleic acids (Asplund et al., 2019). To ensure we were not merely reporting the sequences of
180 the "reagent virome," we performed our wet bench and bioinformatic pipeline on three independent
181 replicates of reagent-only samples. We found no evidence of sequences of any viruses reported here or
182 elsewhere. Further, cross-sample comparison of contigs showed that almost no sequences were found
183 in different animal samples, aside from technical replicates. In total, six viral genomes were observed in
184 multiple unrelated samples from at least two sequencing runs (Table S2). It is unclear whether this small
185 minority of genomes (0.24% of the genomes reported in the current study) represent reagent
186 contamination, lab contamination, or actual presence of the sequences in different types of samples.
187
188 **Assignment of hallmark genes to networks shows expansion of virus sequence space**
189 Single stranded DNA viruses, in general, have vital genes encoding proteins that mediate genome
190 replication, provide virion structure, and, in some cases, facilitate packaging of viral nucleic acid into the
191 virion. Being structurally conserved, these genes also tend to be important for evolutionary comparisons

Supplemental Figure 2: Size distribution of circular DNA sequences from this study

Length, in nucleotides, of circular DNA sequences representing putative viral genomes from this study.

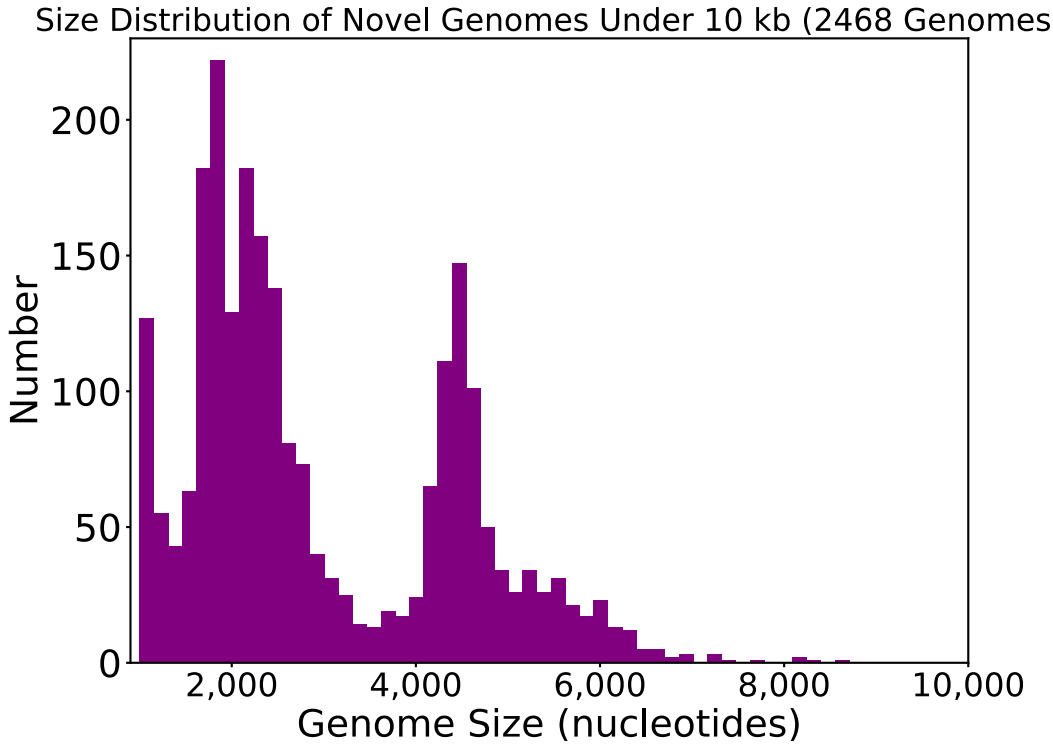

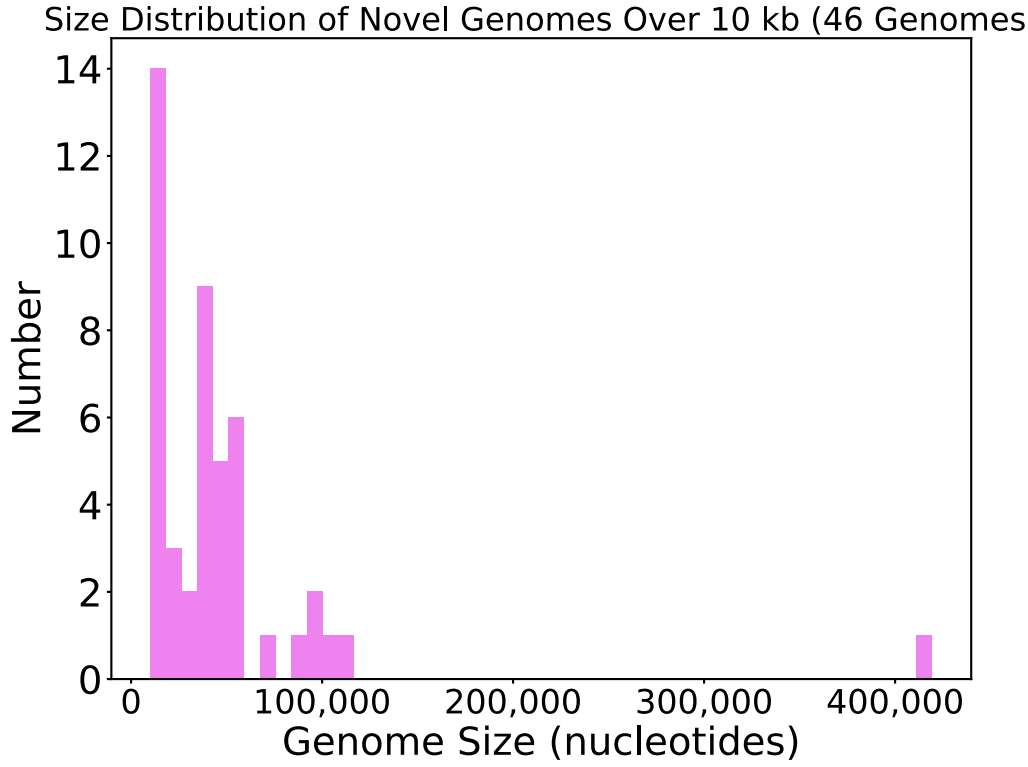

192 and can serve as important "hallmark genes" for virus discovery and characterization. However, even
193 structurally conserved proteins sometimes do not have enough sequence conservation as to be
194 amenable to high confidence BLASTP searches. We therefore set out to catalog hallmark ssDNA virus
195 genes based using protein structural prediction. Structures of hallmark genes of exemplar isolates from
196 most established ssDNA virus families have been solved and deposited in publicly available databases,
197 such as PDB (Protein Data Bank) (Burley et al., 2017). Using bioinformatic tools, such as HHpred, one can
198 assign structural matches for a given gene based on the predicted potential folds of a given amino acid
199 sequence. HHpred has been extensively tested and validated for computational structural modelling by
200 the structural biology community (Meier and Soding, 2015, Huang et al., 2014). The method proves
201 especially useful for protein sequences from highly divergent viral genomes that have little similarity to
202 annotated sequences in current databases.
203 We extracted protein sequences from our dataset and compiled nonredundant proteins from
204 circular ssDNA viruses in GenBank and used them as queries in HHpred searches against the PDB, PFam,
205 and CDD databases. We then grouped structurally identifiable sequences into hallmark gene categories
206 and aligned them pairwise (each sequence was compared to all other sequences) using EFI-EST (Gerlt et
207 al., 2015). The resulting sequence similarity networks (SSNs) were visualized with Cytoscape (Su et al.,
208 2014), with each node representing an predicted protein sequence (Fig. 2-3, Fig. S3). Nodes (sequences)
209 with significant amino acid similarity are connected with lines representing BLAST similarity scores
210 below a threshold E value. Sequence similarity network analyses, it has been proposed (Iranzo et al.,
211 2017), represent relationships between viral sequences better than phylogenetic trees. Further, SSNs
212 have previously been used for viral protein and genome cluster comparison (Bolduc et al., 2017, Lima-
213 Mendez et al., 2008, Lefeuvre et al., 2019, Kazlauskas et al., 2019), and can be used to display related
214 groups of viral genes in two dimensions (Bin Jang et al., 2019). These clusters were also used to guide
215 the construction of meaningful phylogenetic trees (Fig. 2A-B, Fig. S4).
216 In Figure 2, sequences that showed a structural match to a known eukaryotic circular ssDNA
217 virus capsid protein are displayed as a network. This general capsid type features a single beta-jellyroll
218 fold and assembles into T=1 virions of 20-30 nm in diameter. The network shows that sequences from
219 this study expand and link smaller disconnected clusters of sequences found in GenBank entries (Fig. 2A-
220 C). Perhaps more importantly a number of previously unknown clusters were identified, providing
221 insight into highly divergent hallmark sequences and making this capsid sequence space amenable to
222 BLAST searches in GenBank (Fig. 2C). Although the satellite tobacco necrosis virus (STNV) capsid protein
223 encapsidates an RNA molecule, it has previously been noted that its structure is highly similar to the
224 capsid proteins of geminiviruses and other ssDNA viruses (Koonin et al., 2015, Kraberger et al., 2015,
225 Krupovic et al., 2009, Hipp et al., 2017, Bottcher et al., 2004, Zhang et al., 2001) and was included as a
226 model for populating this network.
227 A similar pattern can be seen in sequence similarity networks for the Rep genes of CRESS viruses
228 (Fig. 3). Rep genes have been the primary sequences used for taxonomy of CRESS viruses (Zhao et al.,
229 2019). In this case, it was determined that a network with alignment cutoffs with E values of 1×10^{-60}
230 could split the data neatly into “family-level” clusters (Fontenele et al., 2019, Kraberger et al., 2019),
231 precisely mirroring ICTV taxonomy of CRESS viruses. Many additional family-level clusters can be
232 discerned from unclassified CRESS viruses. Other eukaryotic and prokaryotic ssDNA virus hallmark gene
233 networks are shown in Supplementary Figure 3. Phylogenetic trees of networks from Figure 3 and
234 Supplemental Figure 3 are displayed in Supplemental Figure 4.
235 Cytoscape files of sequence similarity networks and phylogenetic trees can be found at
236 https://ccrod.cancer.gov/confluence/display/LCOTF/DarkMatter.
237
238 **New classes of large CRESS viruses feature unconventional structural genes**

Figure 2: Sequence similarity network analysis of CRESS virus capsid proteins

EFI-EST was used to conduct pairwise alignments of amino acid sequences from this study and GenBank with predicted structural similarity to CRESS virus capsid proteins. The E value cutoff for the analysis was 10-5. (A) Cluster consisting of proteins with predicted structural similarity to geminivirus-like capsids and/or STNV-like capsids. The phylogenetic tree was made from all sequences in this cluster. (B) A cluster consisting of sequences with predicted structural similarity to Circovirus capsid proteins. The phylogenetic tree was made from all sequences in this cluster. (C) Assorted clusters and singletons from unclassified CRESS virus proteins that were modelled to be capsids. (D) Nanovirus capsids. (E) Gyrovirus capsids.

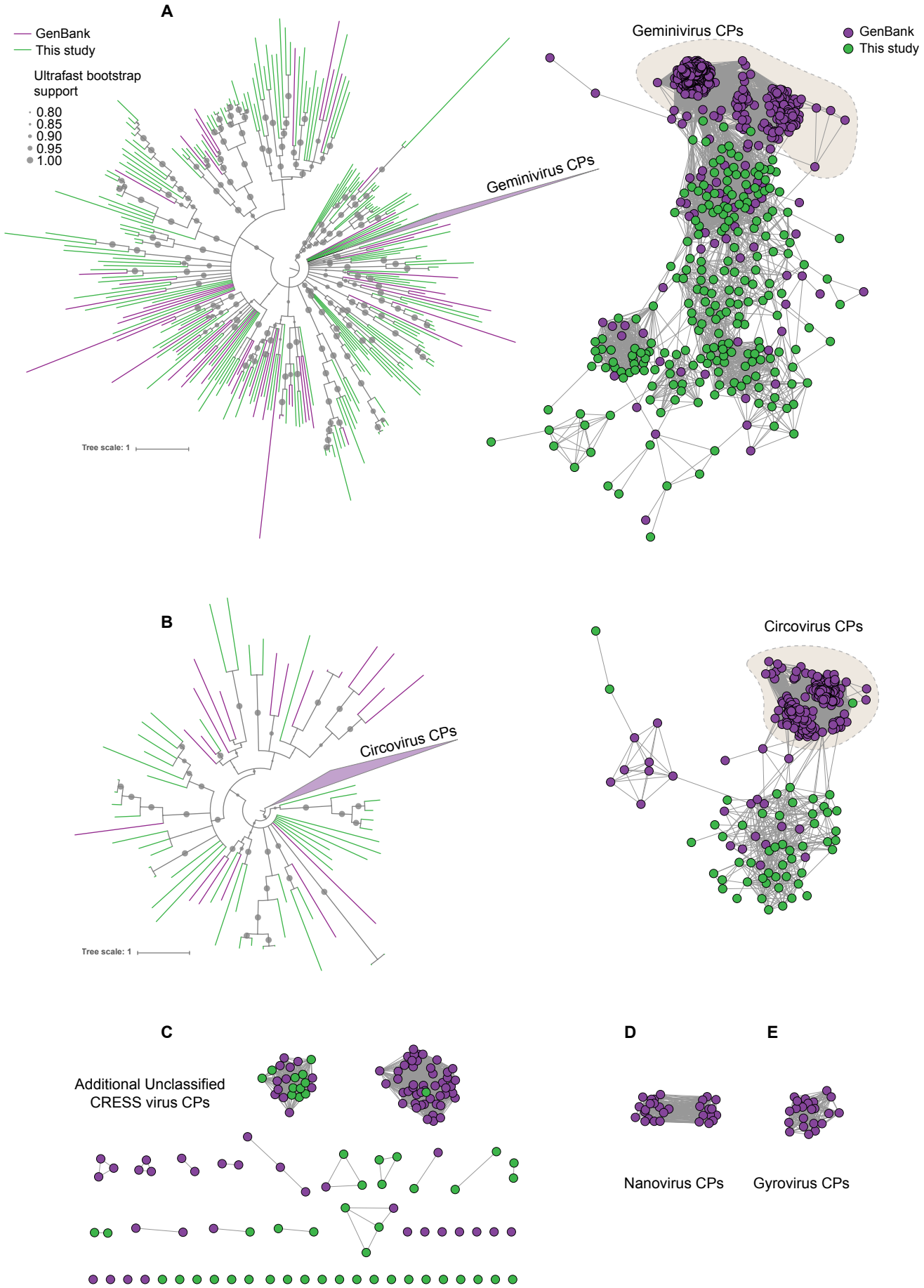

Figure 3: Network analysis of CRESS virus Rep proteins

EFI-EST was used to conduct pairwise alignments of amino acid sequences from this study and GenBank that were structurally modelled to be a rolling-circle replicase (Rep). The analysis used an E value cutoff of 10^{-60} to divide the data into family-level clusters.

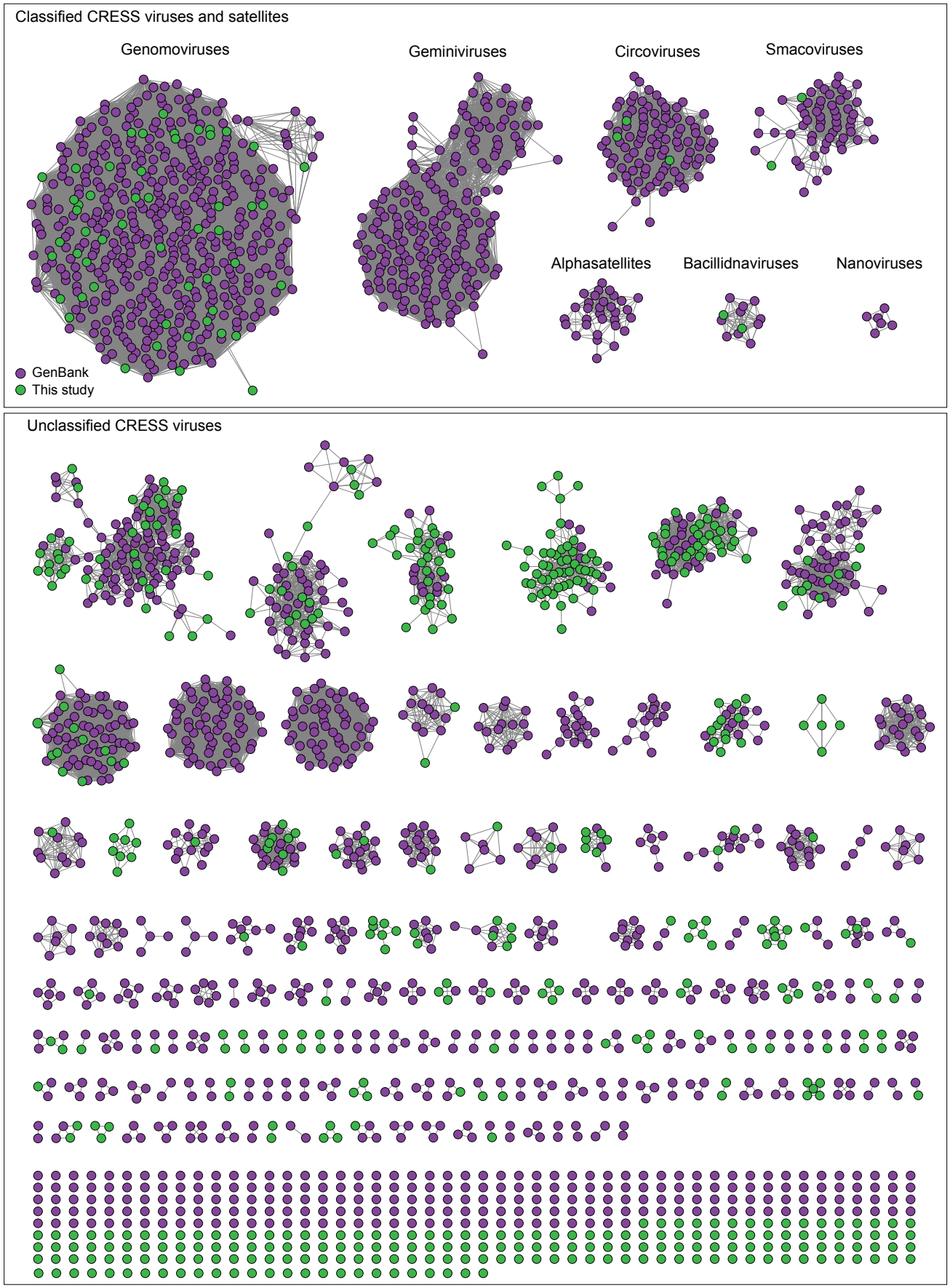

Supplemental Figure 3: Network Analysis of additional viral hallmark genes

Depiction of additional viral hallmark genes from this study and GenBank as sequence similarity networks. E value cutoff = 10^{-5}. See Figure 2 and Methods.

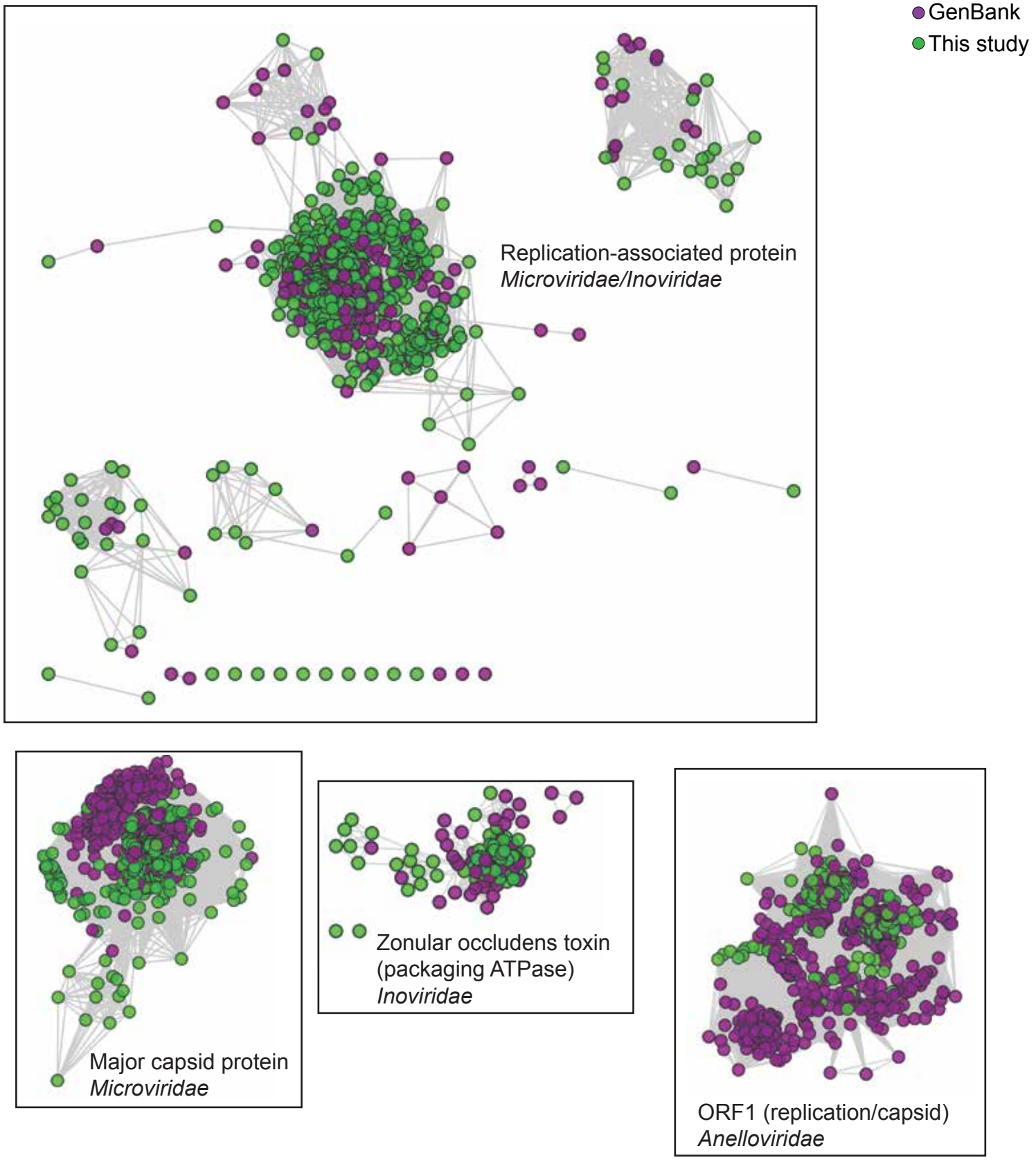

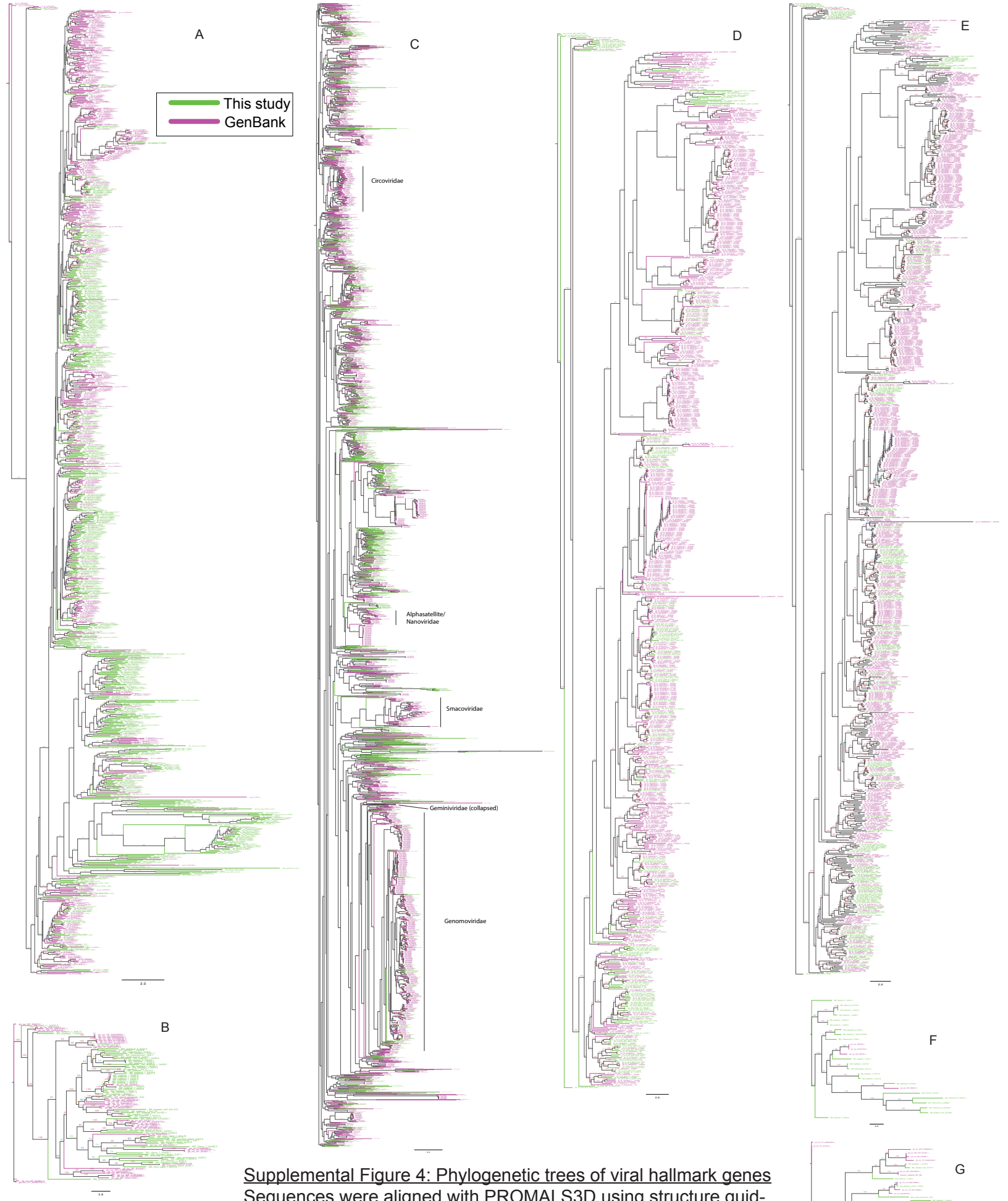

Supplemental Figure 4: Phylogenetic trees of viral hallmark genes
Sequences were aligned with PROMALS3D using structure guidance when possible. Trees were drawn using IQ-Tree with automatic determination of substitution model. See methods. Branches are labeled with bootstrap percent support after 1000 ultrafast bootstrapping events.

239 Although no single family of viruses accounts for the majority of genomes in this study, these results
240 expand the knowledge of the vast diversity of CRESS viruses, which appear to be ubiquitous among
241 eukaryotes (Krupovic et al., 2016, Zerbini et al., 2017, Rosario et al., 2017, Varsani and Krupovic, 2018)
242 and are likely to also infect archaea (Díez-Villaseñor and Rodriguez-Valera, 2019, Kazlauskas et al., 2019).
243 Characterized CRESS viruses have small icosahedral virions (20-30 nm in diameter) with a simple T=1
244 geometry (Khayat et al., 2011). This capsid architecture likely limits genome size, as nearly all previously
245 reported CRESS virus genomes and genome segments are under 3.5 kb. Exceptions to this size rule are
246 bacilladnaviruses, which have 4.5 - 6 kb genomes (Tomaru et al., 2011) and cruciviruses, which have 3.5 -
247 5.5 kb genomes (Quaiser et al., 2016). Interestingly, the genomes of these larger CRESS viruses encode
248 capsid genes that appear to have been acquired horizontally from RNA viruses (Kazlauskas et al., 2017).
249 In our dataset, eight CRESS-like circular genomes exceed 6 kb in length (Fig. 4C-J). Further, this study's
250 large CRESS genomes are apparently attributable to several independent acquisitions of capsid genes
251 from other taxa and/or capsid gene duplication events.
252 Notably, a large CRESS genome (CRESS virus isolate ctdh33, associated with rhabditid
253 nematodes that were serially cultured from a soil sample) encoded three separate genes with structural
254 homology (HHpred probability scores 97-99%) to STNV capsid (Fig 4C). The three predicted STNV capsid
255 homologs in the nematode virus are highly divergent from one another, with only 28-30% amino acid
256 similarity, but also highly divergent from other amino acid sequences in GenBank. A possible explanation
257 for this observation is that the capsid gene array is the result of gene duplication events.
258 To further characterize the soil nematode virus, the three candidate capsid proteins were
259 overexpressed in combination in human-derived 293TT cells (Buck et al., 2004). Particles apparently
260 composed of all three capsid proteins were able to sediment in Optiprep gradients. Further, analysis by
261 negative stain electron microscopy (EM) revealed ~50 nm particles (Fig S5A). Interestingly these particles
262 were found to contain nonspecific nuclease-resistant RNA (Fig S5B). This supports the concept that
263 CRESS virus capsid proteins might theoretically be re-targeted to packing RNA virus genomes or vice
264 versa.
265 CRESS genomes ctba10, ctcc19, ctbj26, ctcd34, and ctbd1037 (ranging from 3.5 - 6.2 kb in
266 length) also each encode two divergent capsid gene homologs (Fig. 4D, Fig S6). Single genomes encoding
267 multiple capsid genes with related but distinct amino acid sequences have been observed in RNA viruses
268 (Agranovsky et al., 1995) and giant dsDNA viruses (Schulz et al., 2017), but we believe that this is the
269 first time it has been reported in ssDNA viruses.
270 Two related large CRESS viruses (ctdb796 and ctce741) encode capsid proteins similar to those
271 of bacilladnaviruses (Fig 4G,I). Interestingly, the Rep genes of the two viruses do not show close
272 similarity to known bacilladnavirus Reps and are instead similar to the Reps of certain unclassified CRESS
273 viruses, suggesting that CRESS ctdb796 and CRESS ctce741 are representatives of a new hybrid CRESS
274 virus family.
275 Two other CRESS virus genomes (isolates ctca5 and ctgh4) encode capsid genes that show amino
276 acid similarity to distinct groups of icosahedral T=3 ssRNA virus capsids (Makino et al., 2013) (tombus-
277 and tombus-like viruses), but not to cruciviruses or bacilladnaviruses (Fig 4A,F, Fig. 5). Further, a 6.6 kb
278 CRESS virus (isolate ctbd466) (Fig 4H) was found to encode a gene with some similarity to the capsid
279 region of the polyprotein of two newly described ssRNA viruses (ciliovirus and brinovirus (Fig. S7B)
280 (Makino et al., 2013, Greninger and DeRisi, 2015). Protein fold predictor Phyre[2] (Kelley et al., 2015)
281 showed a top hit (58% confidence) for the capsid protein of a norovirus (ssRNA virus with T=3
282 icosahedral capsid) for isolate ctbd466 (see GenBank: AXH73946).
283 Two CRESS genomes (ctbe30 and ctbc27) from separate Rhesus macaque stool samples combine
284 Rep genes specific to CRESS viruses with several genes specific to inoviruses, including inovirus-like
285 capsid genes, which encode proteins that form a filamentous virion (Fig 4B, J). The bacteriophage

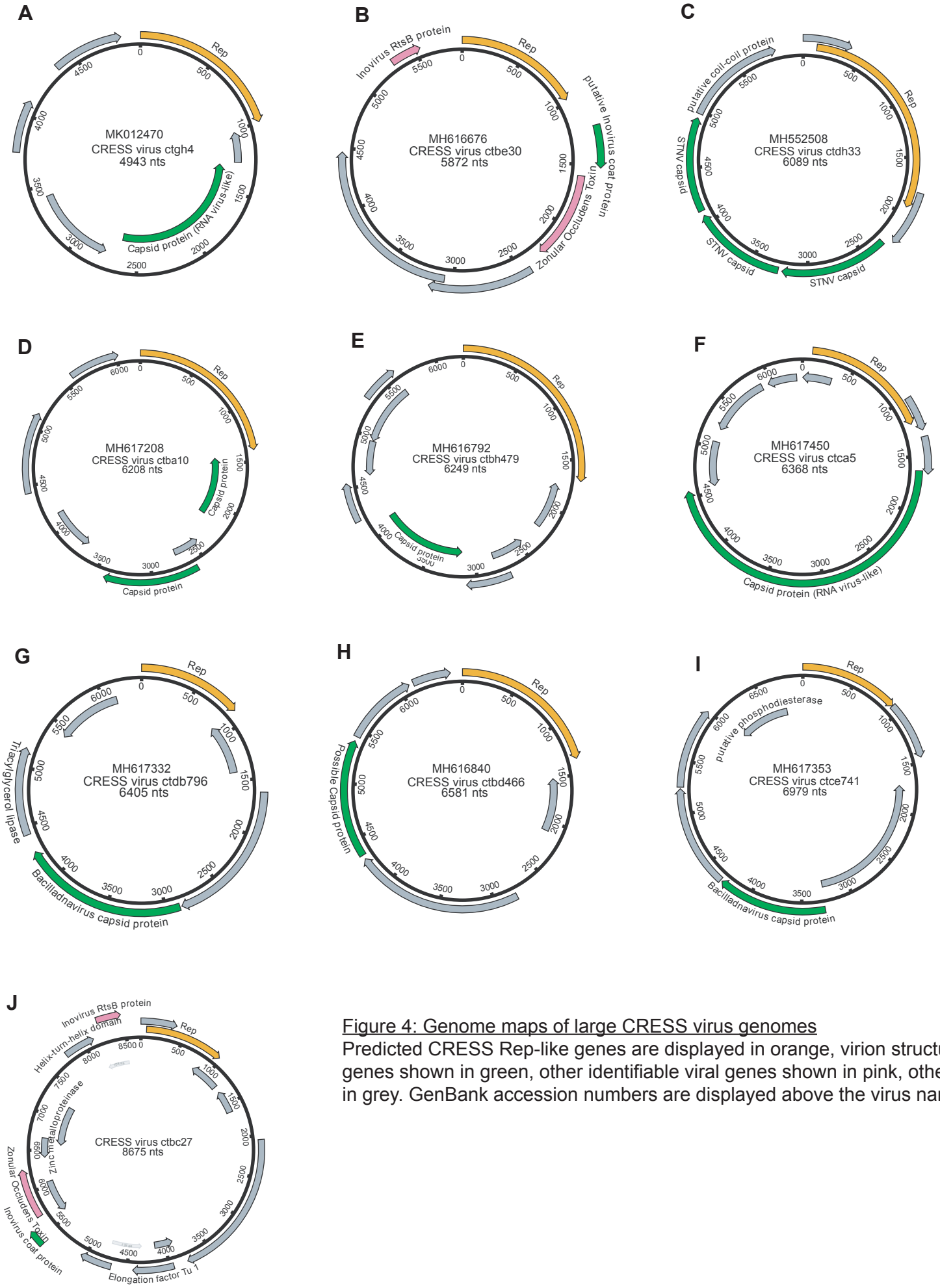

Figure 4: Genome maps of large CRESS virus genomes

Predicted CRESS Rep-like genes are displayed in orange, virion structural genes shown in green, other identifiable viral genes shown in pink, other genes in grey. GenBank accession numbers are displayed above the virus name.

Supplemental Figure 5: Nematode-associated virus capsid expression

Putative capsid proteins from CRESS virus ctdh33 associated with rhabditid nematodes (see Fig. 3) were expressed in a human cell line. (A) Negative Stain EM images of virus-like particles resulting from the expression of all three genes predicted to encode STNV-like capsid proteins. (B) Agarose gel electrophoretic analysis of nucleic acids extracted from ctdh33 VLPs shows that purified VLPs from fraction 4 of the Optiprep gradient contain encapsidated RNA. Note that Benzonase digests both DNA and RNA, DnaseI only digests DNA and Rnase only digests RNA.

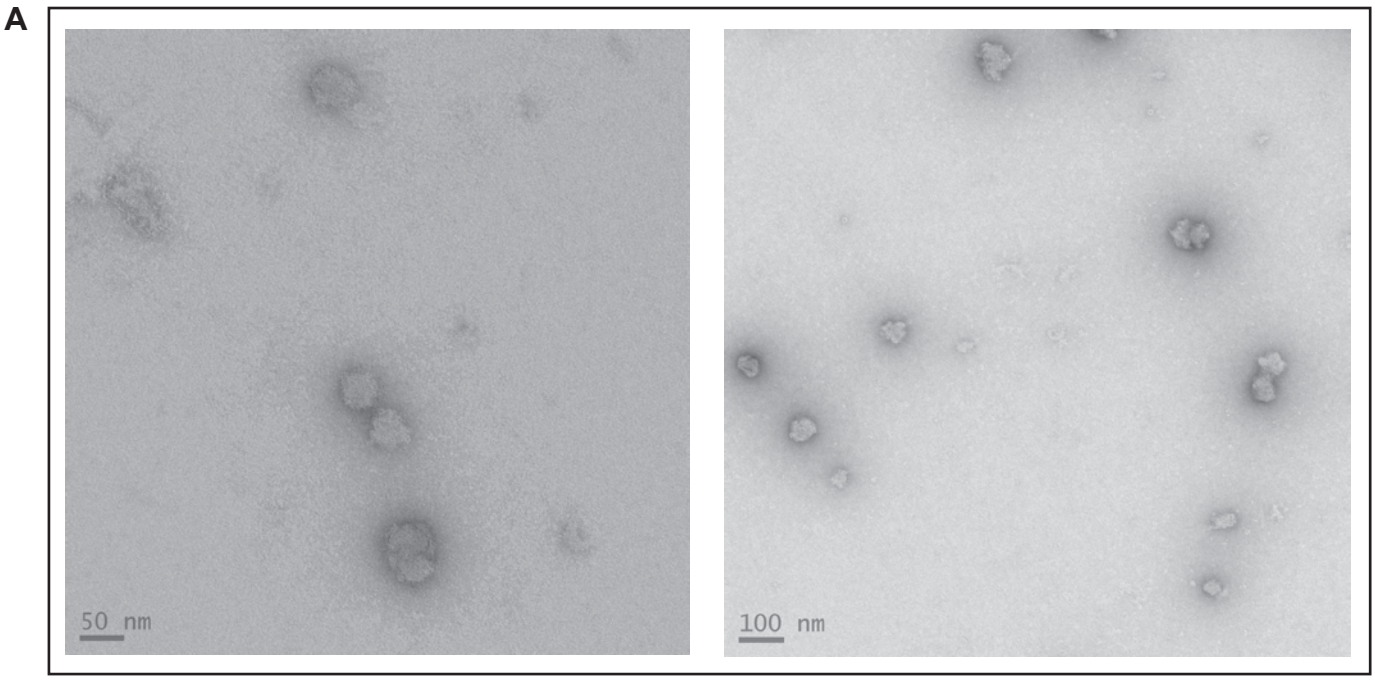

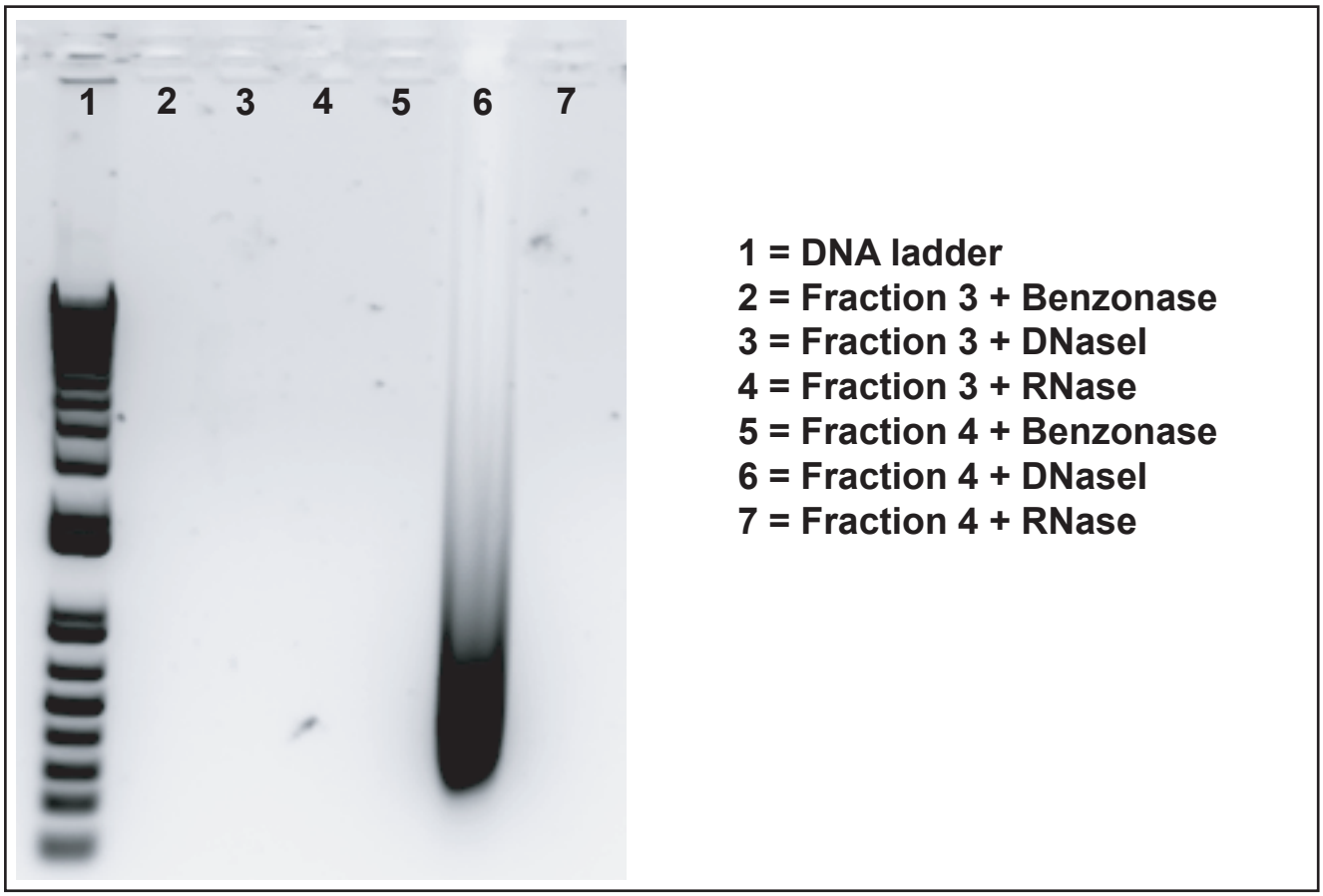

Supplemental Figure 6: Genome maps of additional CRESS genomes encoding multiple capsid genes
CRESS Rep genes are shown in orange, predicted virion structural genes in green, other candidate genes in gray.

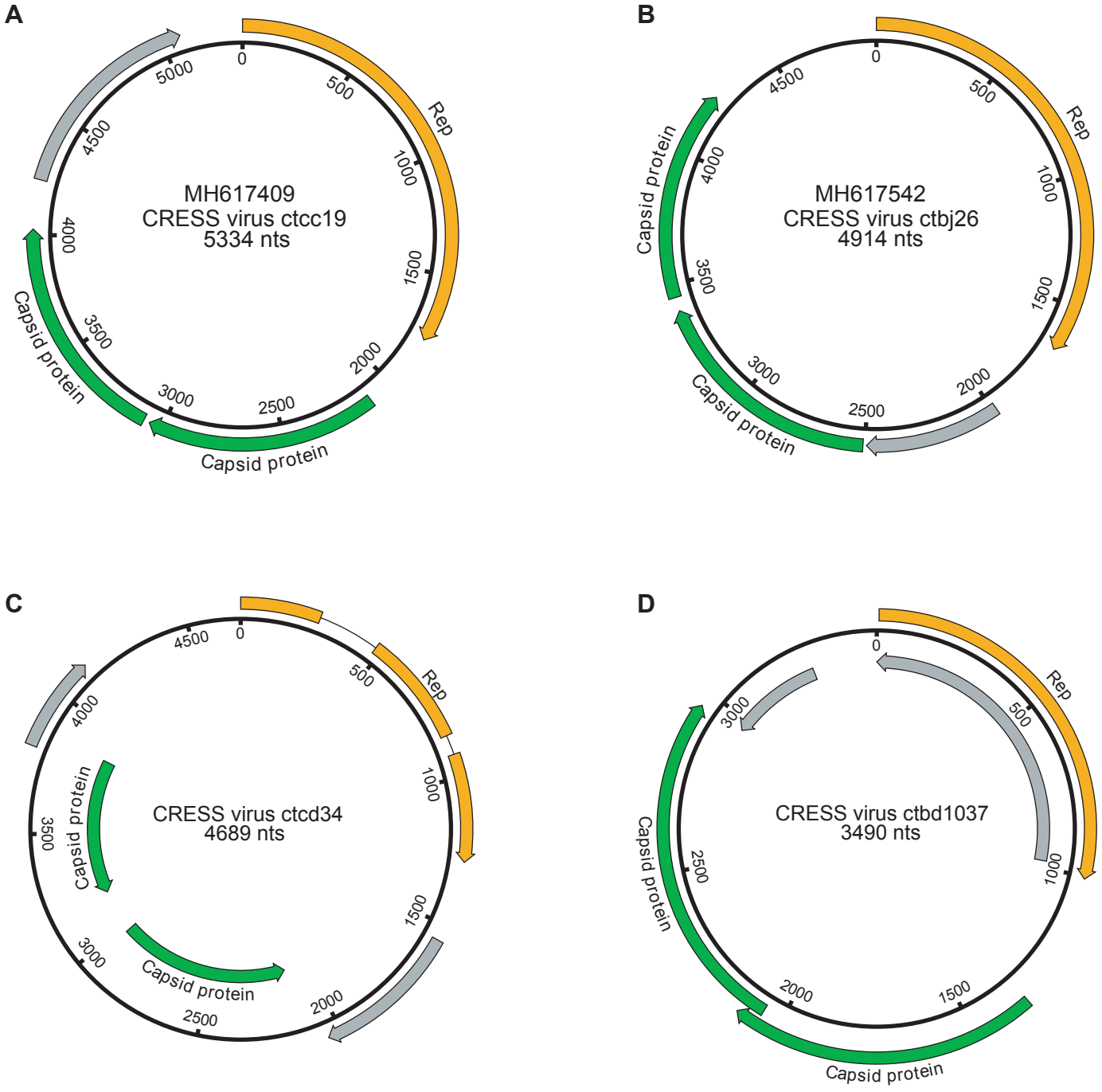

Figure 5: RNA virus capsid-like proteins

Sequence similarity network generated with EFI-EST (E value cutoff of 10-5) showing capsid protein sequences of select ssRNA viruses (Nodaviridae, Tombusviridae, tombus-like viruses) and ssDNA viruses (Bacilladnaviridae and crucivirus) together with protein sequences from DNA virus genomes observed in the present study with predicted structural similarity to an RNA virus capsid protein domain (PDB: 2IZW). Predicted capsid proteins for CRESS virus ctca5 and CRESS virus ctgh4 have no detectible similarity to any known DNA virus sequences. On the left, a phylogenetic tree representing the large cluster is displayed. Collapsed branches consist of Tombusviridae, tombus-like viruses, and Nodaviridae capsid genes.

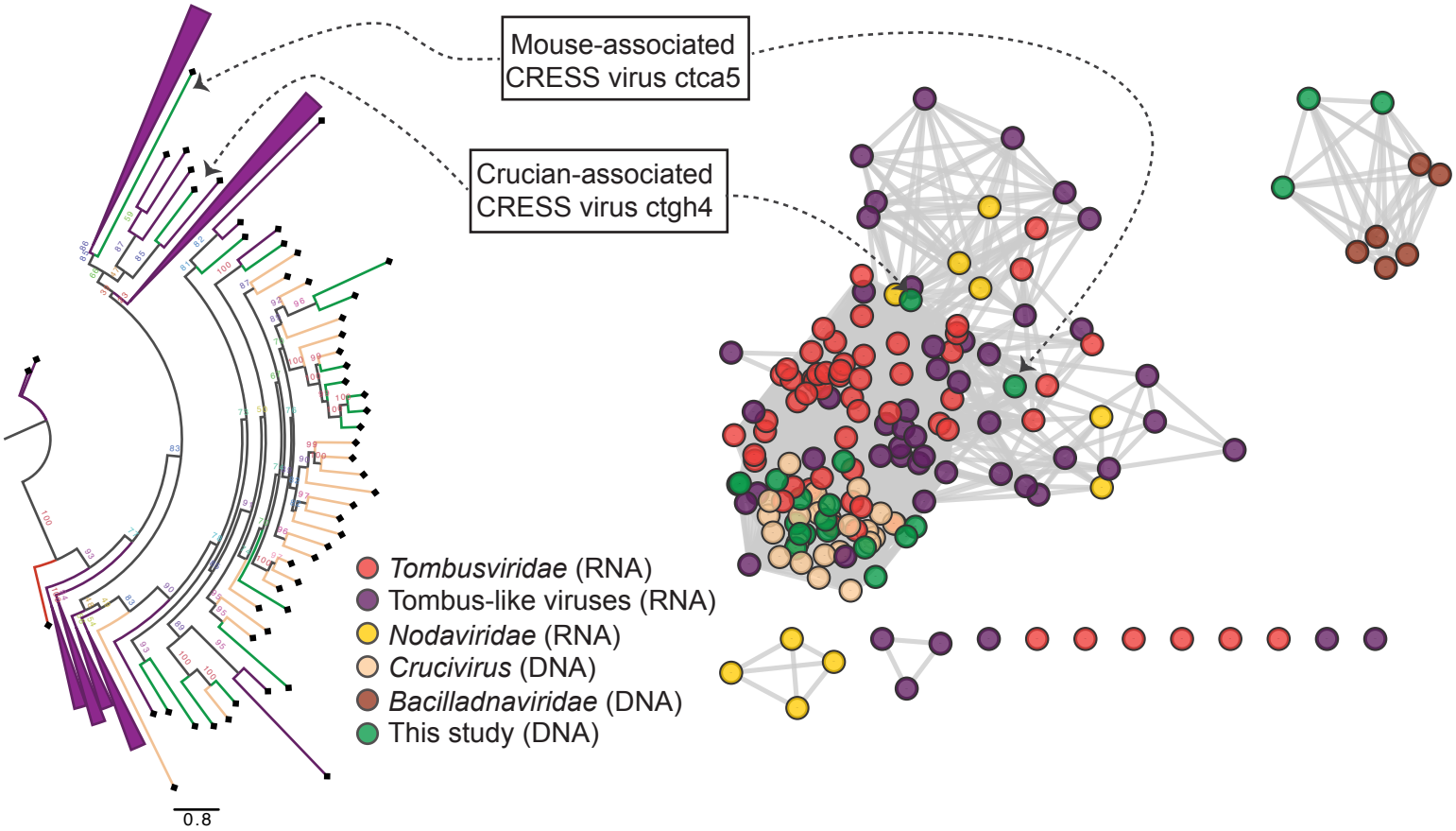

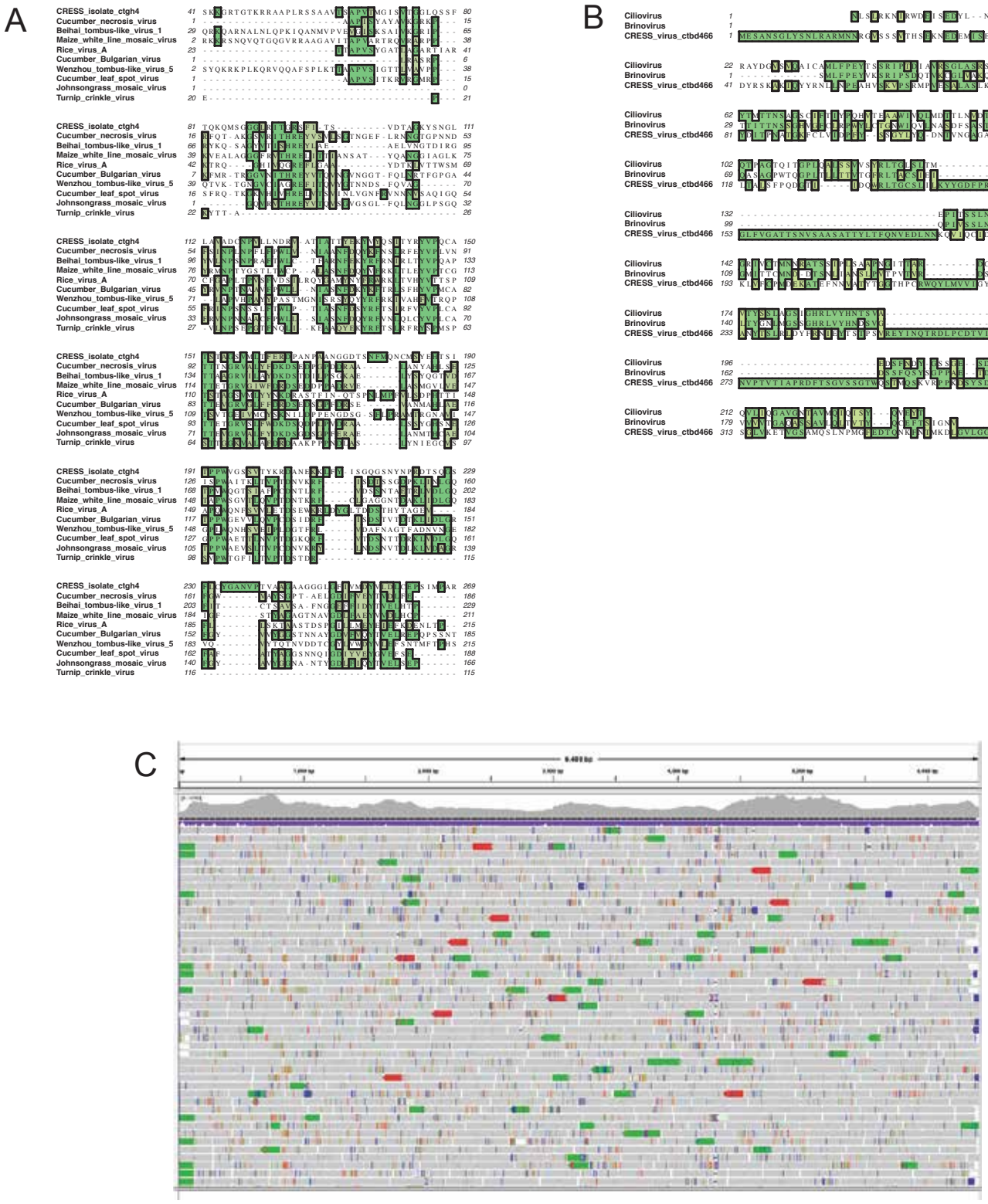

Supplemental Figure 7: Validation of proteins with predicted similarity to RNA virus capsid proteins
(A) First order neighbors for Crucian-associated CRESS virus ctgh4 capsid protein were extracted from the network shown in Figure 5 and aligned using Muscle. (B) The same approach was applied to CRESS virus ctbd466 capsid protein. (C) A visualization (Integrative Genomics Viewer) of a read alignment to CRESS virus isolate ctca5. The visualization shows no evidence of artifactual chimerization in the contig assembly process.

286 families *Inoviridae* and *Microviridae* are ssDNA viruses that replicate via the rolling circle mechanism,
287 but they are not considered conventional CRESS viruses because they infect prokaryotes and do not
288 encode Rep genes with CRESS-like sequences. Other inovirus-like genes encoded in the ctbe30 and
289 ctbc27 genomes include homologs of zonular occludens toxin (ZOT, a packaging ATPase) and RstB (a
290 DNA-binding protein required for host genome integration) (Falero et al., 2009) (Fig 4B, J). TBLASTX
291 searches using ctbe30 and ctbc27 sequences yielded large segments of similarity to various bacterial
292 chromosomes (e.g., GenBank accession numbers AP012044 and AP018536), presumably representing
293 integrated prophages. This suggests that ctbb30 and ctbc27 represent a previously undescribed
294 bacteria-tropic branch of the CRESS virus supergroup.
295 Viral genomes discussed in this section were validated by aligning individual reads back to the
296 contigs followed by visual inspection. No disjunctions were detected, indicating that illegitimate
297 recombinations are not evident (see Fig. S7C for an example).
298
299 **Network analysis of genetic "dark matter" demonstrates conservation of gene sequence and genome**
300 **structure**
301 We defined potential viral "dark matter" in the survey as circular contigs with no hits with E values
302 $<1\times10^{-5}$ in BLASTX searches of a database of viral and plasmid proteins. We posited that leveraging
303 sequence similarity networks would be useful both for analyzing groups of gene homologs and for
304 discerning which gene combinations tended to be present on related circular genomes. To categorize
305 the 609 dark matter elements based on their predicted proteins, we used pairwise comparison with EFI-
306 EST. A majority of translated gene sequences could be categorized into dark matter protein clusters
307 (DMPCs) containing four or more members (Fig. 6A). Further, groups of related dark matter elements
308 (i.e. dark matter genome groups (DMGGs)), much like viral families, could be delineated by the presence
309 of a conserved, group-specific marker gene. For example, DMPC1 can be thought of as the marker gene
310 for DMGG1. Certain DMPCs tend to co-occur on the same DMGG. For instance, DMPC7 and DMPC17
311 ORFs are always observed in genomes with a DMPC1 ORF (i.e., DMGG1) (Fig. 6B). This *pro tempore*
312 categorization method is useful for visualizing the data, but we stress that is not necessarily
313 taxonomically definitive.
314 HHpred, was again employed to make structural predictions for these data (Zimmermann et al.,
315 2018). Instead of querying individual sequences, alignments were prepared using MAFFT (Katoh and
316 Standley, 2013) for each major DMPC to identify conserved residues and increase sensitivity. Then, each
317 alignment was used for an HHpred query. The results indicate that ten DMPCs are likely viral capsid
318 proteins and 11 are rolling circle replicases (Fig. 6A).
319 While most of the circular dark matter in the survey could be characterized using these
320 methods, dark matter contigs represent a small remaining fraction in some samples (Fig. S9).
321
322 **Cell culture expression of candidate "dark matter" capsids yields particles**
323 In contrast to viral genes such as Rep with conserved enzymatic functions, sequences of the
324 capsid genes are often poorly conserved, even within a given viral family (Buck et al., 2016). Moreover, it
325 appears that capsid proteins have arisen repeatedly through capture and modification of different host
326 cell proteins (Krupovic and Koonin, 2017). This makes it challenging to detect highly divergent capsid
327 proteins using alignment-based approaches or even structural modelling. We therefore turned to an
328 alignment-independent approach known as iVireons, an artificial neural network trained by comparing
329 alignment-independent variables between a large set of known viral structural proteins and known non-
330 structural proteins (Seguritan et al., 2012) (https://vdm.sdsu.edu/ivireons/). As an example of the

Figure 6: Dark matter analysis

(A) Sequence similarity network analysis for genes from dark matter circular sequences (minimum cluster size = 4). Clusters are colored based on assigned dark matter genome group (DMGG). Structural predictions from HHpred are indicated (>85% probability). Rep = rolling circle replicases typical of CRESS viruses or ssDNA plasmids. Capsid = single-jellyroll capsid protein. Attachment = cell attachment proteins typical of inoviruses. DNA-Binding = DNA-binding domain. PLA2 = phospholipase A2. FtsL = FtsL-like cell division protein. Clusters that contain a representative protein that was successfully expressed as a virus-like particle are outlined by a dashed rectangle (See Fig. 7). (B) Maps of three examples of DMGG1 with DMPCs labeled (linearized for display). (C) DMGG1 iVireons 'structure' score summary by protein cluster. Scores range from -1 (unlikely to be a virion structural protein) to 1 (likely to be a virion structural protein). Additional iVireons score summaries can be found in Fig. S8.

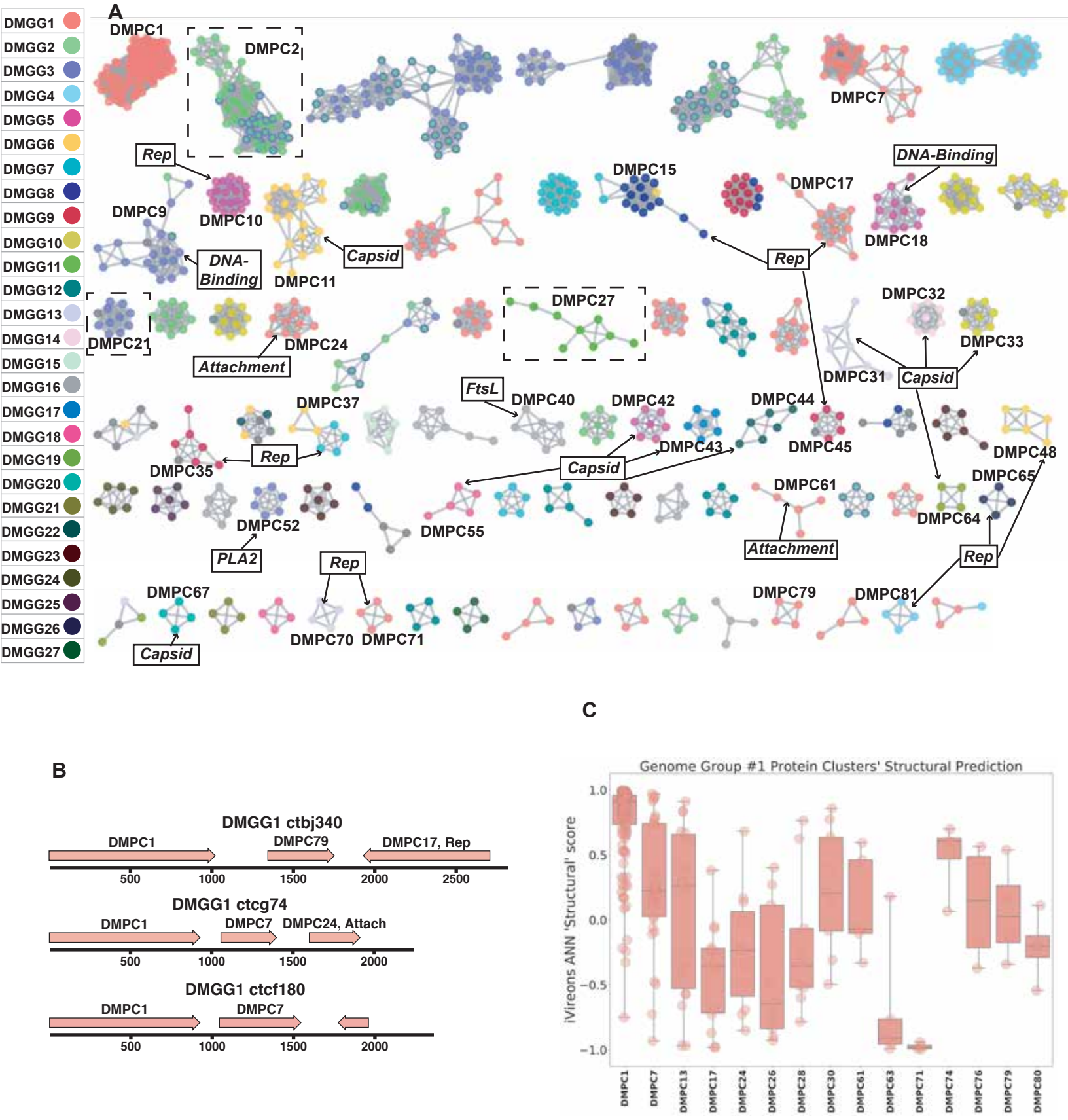

Supplementary Figure 8 (related to Figure 6): iVireons scores of DMGGs with candidate viral structural gene(s)
Box-and-whisker plots of iVireons 'Structural' scores for individual DMPCs (numbers on x-axes) grouped by DMGG. Scores (y-axes) range from -1 (unlikely to be a virion structural protein) to 1 (likely to be a virion structural protein). DMGG2 and DMGG3 have been combined due to inferred chimerism.

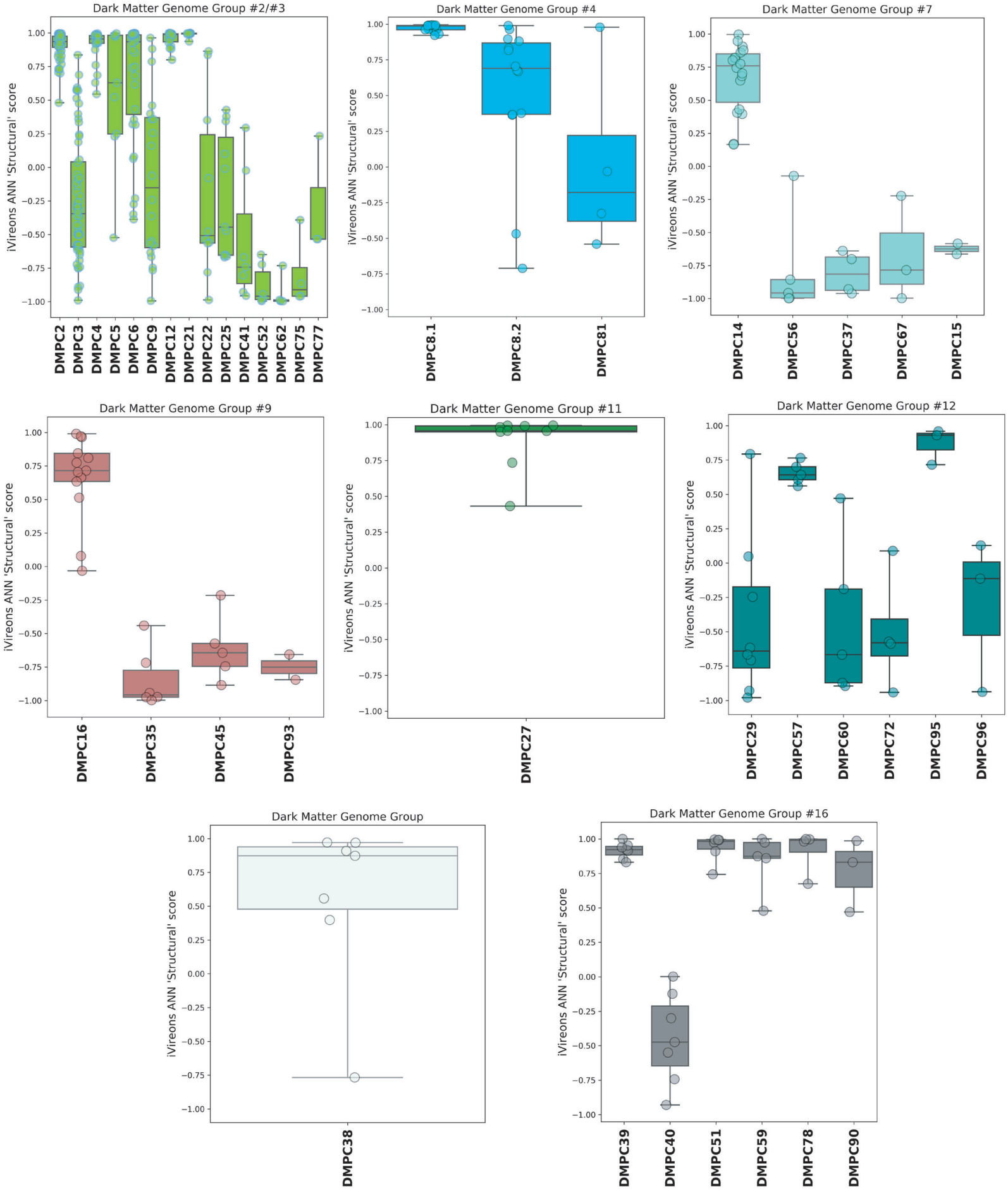

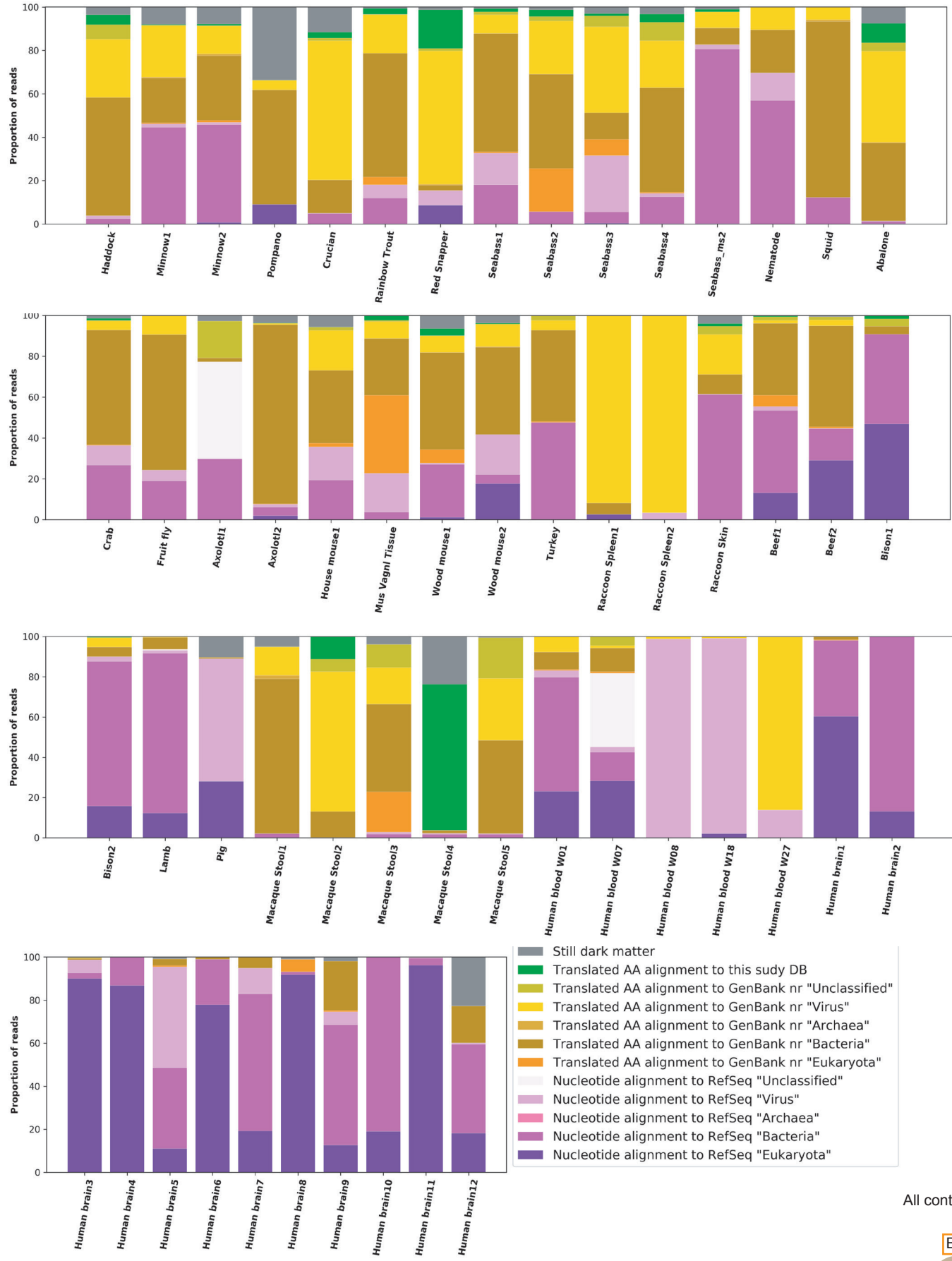

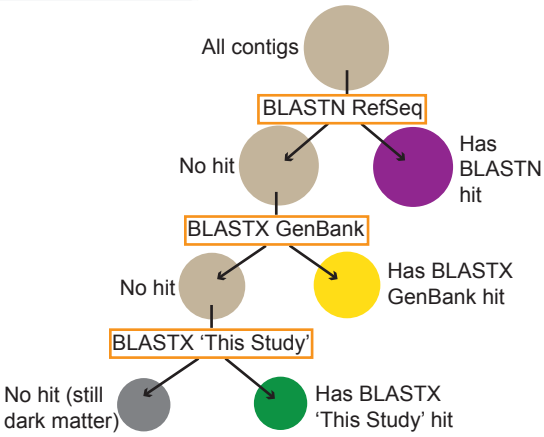

Supplemental Figure 9: Sample characterization by iterative BLAST Searches

Contigs of over 1000 nts from each sample were subject to iterative BLAST searches. First, BLASTN was performed against the RefSeq database. Contigs without hits were then queried by BLASTX against all of GenBank 'nr' database. Contigs without hits were then queried by BLASTX against a database of proteins from genomes reported in this study. The proportion of total reads mapping to each contig was calculated and used for this plot. Individual inspection of contigs shows that most hits in the 'Translated AA alignment to GenBank 'nr' "Bacteria"' were likely plasmid or prophage proteins. The proportions of hits in each category are sensitive to stringency settings and to which databases are chosen for the analysis. The key aims of the figure are to display the proportion of reads the current survey rendered classifiable and the fraction of remaining dark matter reads in various samples.

331 approach, iVireons scores for DMPCs associated with DMGG1 are shown in Fig. 6C. Other sets of
332 iVireons scores can be seen in Fig. S8.
333 Of the 17 DMGGs for which HHPRED did not identify capsid genes, iVireons predicted that ten
334 contain at least one DMPC predicted to encode some type of virion structural protein (median score of
335 cluster >0.70). This allowed us to generate the testable hypothesis that some of these predicted
336 structural proteins would form virus-like particles (VLPs) if expressed in cell culture.
337 A subset of predicted capsid proteins were expressed in 293TT cells and/or in *E. coli* and
338 subjected to size exclusion chromatography. Electron microscopic analysis showed that several of the
339 predicted capsid proteins formed roughly spherical particles, whereas a negative control protein did not
340 form particles (Fig. 7). Although the particles were highly irregular, the DMGC11 isolate ctgh70
341 preparation was found to contain nuclease-resistant nucleic acids, consistent with nonspecific
342 encapsidation. The results suggest that, in multiple cases, we were able to experimentally confirm that
343 iVireons correctly predicted the identity of viral capsid proteins.
344
345 **Discussion**
346 Massive parallel DNA sequencing surveys characterizing microbial communities typically yield a
347 significant fraction of reads that cannot be mapped to known genes. The present study sought to
348 provide the research community with an expanded catalog of viruses with circular DNA genomes
349 associated with humans and animals, as well as a means to characterize future datasets. We hope that
350 the availability of this expanded viral sequence catalog will facilitate future investigation into
351 associations between viral communities and disease states. Our annotation pipeline, Cenote-Taker, can
352 be accessed via http://www.cyverse.org/discovery-environment. The CyVerse version of Cenote-Taker
353 can readily annotate circular or linear DNA viruses. RNA viruses with polyproteins or frameshifts will
354 require *post hoc* manual editing.
355 At the present time, GenBank's RefSeq database includes complete sequences for 8112 viral
356 genomes, most of which fit into 131 families recognized by the International Committee on Taxonomy
357 of Viruses (ICTV) (King et al., 2018). Similarly, the IMG/VR database contains over 14,000 circular virus
358 genomes from hundreds of studies, though some of these appear to be redundant with each other and
359 are not comprehensively annotated (Paez-Espino et al., 2019). The current study, which focused on
360 circular DNA viruses with detergent-resistant capsids, found 2,514 new complete circular genomes. The
361 availability of these comprehensively annotated genomes in GenBank contributes new information and
362 understanding to a broad range of established, emerging, and previously unknown taxa. Figure 3 shows
363 dozens of potential family-level groupings within the unclassified CRESS virus supergroup. Sequences
364 from this study contribute to 40 of such groupings and constitute the only members of seven groups.
365 There are also 192 singleton CRESS sequences that could establish many additional family-level groups.
366 Although small ssDNA viruses are ubiquitous, they are often overlooked in studies that only
367 characterize sequences that are closely related to reference genomes. In addition, ssDNA is not detected
368 by some current DNA sequencing technologies unless second-strand synthesis (such as the RCA
369 approach used in the current study) is conducted.
370 While many of the viruses discovered in this study appear to be derived from prokaryotic
371 commensals, it is important to note that bacteriophages can contribute to human and animal diseases
372 by transducing toxins, antimicrobial resistance proteins, or genes that alter the physiology of their
373 bacterial hosts (Waldor and Mekalanos, 1996). Furthermore, interaction between animal immune
374 systems and bacteriophages appears to be extensive (Hodyra-Stefaniak et al., 2015).
375 Over 100 distinct human anellovirus sequences were found in human blood. Anelloviruses have
376 yet to be causally associated with any human disease, but this study indicates that we are likely still just
377 scratching the surface of the sequence diversity of human anelloviruses. It will be important to fully
378 catalog this family of viruses to address the field's general assumption that they are harmless.

379 Several of the CRESS viruses detected in this study are larger than any other CRESS virus
380 genomes that have been described previously. In some cases, the larger size of these genomes may have
381 been enabled by a process involving capsid gene duplication events. Further, CRESS virus acquisition of
382 T=3 capsids from ssRNA *Nodaviridae* and *Tombusviridae* families has been previously suggested as the
383 origin of bacilladnaviruses (Kazlauskas et al., 2017) and cruciviruses (Steel et al., 2016, Dayaram et al.,
384 2016, Roux et al., 2013, Krupovic et al., 2015), respectively. We present evidence of additional
385 independent recombination events between CRESS viruses and ssRNA viruses and ssDNA
386 bacteriophages. In light of these findings, it should be reiterated that only DNA (not RNA) was
387 sequenced in our approach, so DNA/RNA *in silico* false recombination does not seem plausible. These
388 data suggest that CRESS viruses are at the center of a tangled evolutionary history of viruses in which
389 genomes change not just via gradual point mutations but also through larger scale recombination and
390 hybridization events.
391 It is likely that some dark matter sequences detected in this study share a common ancestor
392 with known viruses but are too divergent to retain discernable sequence similarity. In some cases, the
393 dark matter circles may represent a more divergent segment of a virus with a multipartite genome.
394 Alternatively, some of these sequences likely represent entirely new viral lineages that have not
395 previously been recognized.
396
397 **Methods**
398
399 LEAD CONTACT AND MATERIALS AVAILABILITY
400
401 Further information and requests for resources and reagents should be directed to and will be
402 fulfilled by the Lead Contact, Chris Buck (buckc@mail.nih.gov)
403
404 EXPERIMENTAL MODEL AND SUBJECT DETAILS
405
406 Human-derived 293TT cells (female) were generated in-house (Buck et al., 2004). The cells were not
407 authenticated for this study.
408 T7 Express lysY/I^q *E. coli* were purchased from New England Biolabs.
409
410
411 METHOD DETAILS
412
413 <u>Sample collection and sequencing</u>
414
415 De-identified human swabs and tissue specimens were collected under the approval of various
416 Institutional Review Boards (Supplemental Table 1). Animal tissue samples were collected under the
417 guidance of various Animal Care and Use Committees.
418
419 Nematodes were cultured out of soil samples collected in Bethesda, Maryland, USA on OP50-Seeded
420 NGM-lite plates (*C. elegans* kit, Carolina Biological Supply).
421

422 Viral particles were concentrated by subjecting nuclease-digested detergent-treated lysate to
423 ultracentrifugation over an Optiprep step gradient, as previously described
424 https://ccrod.cancer.gov/confluence/display/LCOTF/Virome (Peretti et al., 2015). Specifically, for each
425 sample, no more than 0.5 g of solid tissue was minced finely with a razorblade. Alternatively, no more
426 than 500 µl of liquid sample was vortexed for several seconds. Samples were transferred to 1.5ml
427 siliconized tubes. The samples were resuspended in 500 µl Dulbecco's PBS and Triton X-100 (Sigma)
428 detergent was added to a final concentration of 1% w/v. 1 µl of Benzonase (Sigma) was added. Samples
429 were vortexed for several seconds. Samples were incubated in a 37ºC water bath for 30 minutes, with
430 brief homogenising using a vortex every 10 minutes. After incubation, NaCl was added to the samples to
431 a final concentration of 0.85M. Tubes were spun for 5 minutes at 5000g. Resulting supernatants were
432 transferred to a clean siliconized tube. Supernatant-containing tubes were spun for an additional 5
433 minutes at 5000g. Resulting supernatants were added to iodixanol/Optiprep (Sigma) step gradients in
434 ultracentrifuge tubes (Beckman: 326819) (equal volumes 27%, 33%, 39% iodixanol with 0.8M NaCl; total
435 tube volume, including sample, ~5.1ml). Ultracentrifuge tubes were spun at 55,000rpm for 3.5 hours
436 (Beckman: Optima L-90K Ultracentrifuge). After spin, tubes were suspended over 1.5ml siliconized
437 collection tubes and pierced at the bottom with 25G needle. Six fractions of equal volume were
438 collected drop-wise from each ultracentrifuge tube.
439 From each fraction, 200 µl was pipette to a clean siliconized tube for virus particle lysis and DNA
440 precipitation. To disrupt virus particles, 50 µl of a 5X master mix of Tris pH 8 (Invitrogen, final conc.
441 50mM), EDTA (Invitrogen, final conc. 25mM), SDS (Invitrogen, final conc. 0.5%), Proteinase K (Invitrogen,
442 final conc. 0.5%), DTT (Invitrogen, final conc. 10mM) was added and mixed by pipetting up and down.
443 Samples were heated at 50ºC for 15 minutes. Then, proteinase K was inactivated for 10 minutes at 72ºC.
444 To the 250 µl of sample, 125 µl of 7.5M ammonium acetate was added and mixed by vortexing. Then,
445 975 µl of 95% ethanol was added and mixed by pipetting. This was incubated at room temperature for 1
446 hour. Then, the samples were transferred to a 4ºC fridge overnight.
447 Samples were then restored to ambient temperature. Then, samples were spun for 1 hour at
448 20,000g in a temperature-controlled tabletop centrifuge set to 21ºC. Supernatant was aspirated, and
449 500 µl ethanol was added to each pellet. Pellets were resuspended by flicking. Then, samples were spun
450 for 30 minutes at 20,000g in a temperature-controlled tabletop centrifuge set to 21ºC. Supernatant was
451 aspirated, and samples were spun once more at 20,000g for 3 minutes. Remaining liquid was carefully
452 removed with a 10 µl micropipette. Tubes were left open and air dried for at least 10 minutes.
453 DNA from individually collected fractions of the gradient was amplified by RCA using phi29 polymerase
454 (TempliPhi, Sigma) per manufacturer's instructions. While we expected most viral particles to travel to
455 the middle of the gradient based on previous experiments, RCA was conducted on individual fractions
456 spanning the gradient, in an attempt to detect viruses with different biophysical properties (Kauffman et
457 al., 2018). Pooled, amplified fractions were prepared for Illumina sequencing with Nextera XT kits. Then
458 libraries were sequenced with Illumina technology on either MiSeq or NextSeq500 sequencers. Contigs
459 were assembled using SPAdes with the 'plasmid' setting. Circularity was confirmed by assessing
460 assembly graphs using Bandage (Wick et al., 2015).
461
462 Analysis of brain samples

463 Brain samples were initially analyzed by Optiprep gradient purification, RCA amplification, and deep
464 sequencing, as described above. JC polyomavirus, which has previously been reported in brain samples
465 (Chalkias et al., 2018), can display high buoyancy in Optiprep gradients (Geoghegan et al., 2017).
466 Fractions from near the top of the Optiprep gradient were subjected to an alternative method of virion
467 enrichment using microcentrifuge columns (Pierce) packed with 2 ml of Sepharose 4B Bead suspension
468 (Sigma) exchanged into PBS. Fractions were clarified at 5000 x g for 1 minute, and 200 µl of clarified
469 extract was loaded onto the gel bed. The column was spun at 735 x g and the eluate was digested with
470 proteinase K, ethanol-precipitated, and subjected to RCA. No additional viral sequences were detected
471 by this method.
472
473 The brain samples were also subjected to confirmatory analysis by RNA sequencing. RNA was extracted
474 from brain tissues with Qiagen Lipid Tissue RNeasy Mini Kit and subjected to human ribosomal RNA
475 depletion with Thermo RiboMinus. The library was prepared with NEBNext Ultra™ II Directional RNA
476 Library Prep Kit for Illumina and subjected to massive parallel sequencing on the Illumina HiSeq platform
477 (see BioProject PRJNA513058).
478
479 Cenote-Taker, Virus Discovery and Annotation Pipeline
480 Cenote-Taker, a bioinformatics pipeline written for this project and fully publicly available on CyVerse,
481 was used for collection and detailed annotation of each circular sequence. The flow of the program can
482 be described as follows:
483 (1) Identifies and collects contigs (assembled with SPAdes) larger than 1000 nts
484 (2) Predicts which contigs are circular based on overlapping ends
485 (3) Determines whether circular contig has any ORFs of 80 AA or larger or else discards sequence
486 (4) Uses BLASTN against GenBank 'nt' database to disregard any circular sequences that are >90%
487 identical to known sequences across a >500 bp window
488 (5) Uses Circlator (Hunt et al., 2015) to rotate circular contigs so that a non-intragenic start codon of one
489 of the ORFs will be the wrap point
490 (6) Uses BLASTX against a custom virus + plasmid database (derived from GenBank 'nr' and RefSeq) to
491 attempt to assign the circular sequence to a known family
492 (7) Translates each ORF of 80 AA or larger
493 (8) Uses RPS-BLAST to predict function of each ORF by aligning to known NCBI Conserved Domains
494 (9) Generates a tbl file of RPS-BLAST results
495 (10) Takes ORFs without RPS-BLAST hits and queries the GenBank 'nr viral' database with BLASTP
496 (11) Generates a tbl file of BLASTP results
497 (12) Takes ORFs without any BLASTP hits and queries HHblits (databases: uniprot20, pdb70, scop70,
498 pfam_31, NCBI_CD)
499 (13) Generates a tbl file of HHblits results
500 (14) Complies with a GenBank request to remove annotations for ORFs-within-ORFs that do not contain
501 conserved sequences
502 (15) Combines all tbl files into a master tbl file
503 (16) Generates a unique name for each virus based on taxonomic results
504 (17) Generates properly formatted fsa and tbl files in a separate directory

505 (18) Uses tbl2asn to make gbf (for viewing genome maps) and sqn files (for submission to GenBank)
506
507 The source code can be found at: https://github.com/mtisza1/Cenote-Taker
508
509 This work utilized the computational resources of the NIH HPC Biowulf cluster. (http://hpc.nih.gov).
510
511 Genome maps were drawn, and multiple sequence alignments were computed and visualized using
512 MacVector 16.
513
514 Anelloviruses
515 Analysis of linear contigs in the survey found many instances of recognizable viral sequences. One
516 noteworthy example were anelloviruses, where many contigs terminated near the GC-rich stem-loop
517 structure that is thought to serve as the origin of replication. This segment of the anellovirus genome is
518 presumably incompatible with the short read deep sequencing technologies used in this study. Nearly
519 complete anellovirus genomes, defined as having a complete ORF1 gene and at least 10-fold depth of
520 coverage, were also deposited in GenBank (Table S1).
521
522 GenBank Sequences
523 Amino Acid sequences from ssDNA viruses were downloaded in June 2018 based on categories in the
524 NCBI taxonomy browser. As many sequences in GenBank are from identical/closely related isolates, all
525 sequences were clustered at 95% AA ID using CD-HIT (Fu et al., 2012).
526
527 Sequence Similarity Networks
528 Amino acid sequences from GenBank (see above) and this study were used as queries for HHsearch (the
529 command-line iteration of HHpred) against PDB, PFam, and CDD. Sequences that had hits in these
530 databases of 80% probability or greater were kept for further analyses. Note that capsid protein models
531 for some known CRESS virus families have little, if any, similarity to other capsid sequences and have not
532 been determined (e.g. *Genomoviridae* and *Smacoviridae*) and were therefore not displayed in networks.
533 Models used: (CRESS virus capsids network:5MJF_V, 3R0R_A, 5MJF_Ba, 4V4M_R, 4BCU_A, PF04162.11,
534 5J37_A, 5J09_C, 3JCI_A, cd00259, PF04660.11, PF03898.12, PF02443.14, pfam00844); (CRESS virus Rep
535 network:4PP4_A, 4ZO0_A, 1M55_A, 1UUT_A, 1U0J_A, 1S9H_A, 4R94_A, 4KW3_B, 2HWT_A, 1L2M_A,
536 2HW0_A, PF08724.9, PF17530.1, PF00799.19, PF02407.15, pfam08283, PF12475.7, PF08283.10,
537 PF01057.16, pfam00799); (*Microviridae*/*Inoviridae* replication-associated protein: 4CIJ_B, 4CIJ_C,
538 PF05155.14, PF01446.16, PF11726.7, PF02486.18, PF05144.13, PF05840.12); (*Microviridae* capsid:
539 1M06_F, 1KVP_A, PF02305.16); (*Anelloviridae* ORF1: PF02956.13); (*Inoviridae* ZOT: 2R2A_A,
540 PF05707.11).
541
542
543 Phylogenetic Trees
544 Sequences from this study and GenBank were grouped by structural prediction using HHpred. Then,
545 sequences were compared by EFI-EST to generate clusters with a cut-off of $1x10^{-5}$. Sequences from
546 these clusters were then extracted and aligned with PROMALS3D (Pei and Grishin, 2014) using structure

547 guidance, when possible. Structures used: (*Microviridae* MCP: 1KVP); (CRESS virus capsid STNV-like:
548 4V4M); (CRESS virus capsid circo-like: 3JCI); (*Inoviridae* ZOT: 2R2A); (CRESS virus Rep: 2HW0) (CRESS
549 virus/RNA virus S Domain capsid: 2IZW). The resulting alignments were used to build trees with IQ-Tree
550 with automatic determination of the substitution model and 1000 ultrafast bootstraps (Nguyen et al.,
551 2015). Models used: (*Microviridae* MCP: Blosum62+F+G4); (*Microviridae* Rep I: Blosum62+I+G4);
552 (*Microviridae* Rep II: LG+I+G4); (*Microviridae* Rep III: VT+I+G4); (CRESS virus/RNA virus S Domain capsid:
553 Blosum62+F+G4); (*Circoviridae* capsid: VT+F+G4); (CRESS virus capsid STNV-like: VT+F+G4); (*Inoviridae*
554 ZOT: VT+I+G4); (*Anelloviridae* ORF1: VT+F+G4). Trees were visualized with FigTree
555 (http://tree.bio.ed.ac.uk/software/figtree/) and iTOL (Letunic and Bork, 2019).
556
557 Expressing Potential Viral Structural Proteins in human 293TT cells
558 Codon-modified expression constructs encoding the three predicted STNV-like capsid proteins from the
559 nematode virus (CRESS virus isolate ctdh33) were designed according to a previously reported "as
560 different as possible" algorithm
561 https://ccrod.cancer.gov/confluence/display/LCOTF/Pseudovirus+Production. 293TT cells were
562 transfected with combinations of STNV capsid-like protein expression constructs for roughly 48 hours.
563 Cells were lysed in a small volume of PBS with 0.5% Triton X-100 or Brij-58 and Benzonase (Sigma). After
564 several hours of maturation at neutral pH, the lysate was clarified at 5000 x g for 10 min. The clarified
565 lysate was loaded onto a 27-33-39% Optiprep gradient in PBS with 0.8 M NaCl. Gradient fractions were
566 collected by bottom puncture of the tube and screened by PicoGreen nucleic acid stain (Invitrogen),
567 BCA, and SDS-PAGE analysis. Electron microscopic analysis was then performed. Expression in 293TT
568 cells of some "dark matter" virus capsids was attempted but not successful in any case.
569
570 Expressing Potential Viral Structural Proteins in *E. coli*
571 Several genes that were identified by iVireons as being potential viral structural proteins were cloned
572 into plasmids with a T7 polymerase-responsive promoter. Plasmids were transfected into T7 Express
573 lysY/I^q *E. coli*, which express T7 polymerase under the induction of IPTG. Bacteria were grown at 37ºC in
574 LB broth until OD600 = 0.5. Flasks were cooled to room temperature, IPTG was added to 1 mM, and
575 cultures were shaken at room temperature for approximately 16 hours. Cells were then pelleted for
576 immediate processing.
577 Total protein was extracted with a BPER (Pierce) and nuclease solution. Then, virion-sized particles were
578 enriched from the clarified lysate using size exclusion chromatography with 2% agarose beads
579 https://ccrod.cancer.gov/confluence/display/LCOTF/GelFiltration. Fractions were analyzed using
580 Coomassie-stained SDS-PAGE gels for presence of a unique band corresponding to the expressed
581 protein. Fractions of interest were analyzed using negative stain electron microscopy.
582
583 Electron Microscopy
584 Five µl samples were adsorbed onto a carbon-deposited copper grid for one minute. Sample was then
585 washed 5 times on water droplets then stained with 0.5% uranyl acetate for 1 second. The negatively
586 stained samples were examined on a FEI Tecnai T12 transmission electron microscope.
587
588 Sequencing

589 Illumina sequencing was conducted at the CCR Genomics Core at the National Cancer Institute,
590 NIH, Bethesda, MD 20892.
591
592 DATA AND CODE AVAILABILITY
593
594 All reads and annotated genomes associated with this manuscript can be found on NCBI BioProject
595 Accessions PRJNA393166 and PRJNA396064.
596
597 Cenote-Taker, the viral genome annotation pipeline, can be used by interested parties on the Cyverse
598 infrastructure: http://www.cyverse.org/discovery-environment.
599
600 ADDITIONAL RESOURCES
601
602 Relevant protocols on lab website: https://ccrod.cancer.gov/confluence/display/LCOTF/Virome
603
604 **Acknowledgements**
605
606 This research was supported [in part] by the Intramural Research Program of the NIH, National Cancer
607 Institute.
608 We would like to acknowledge the GenBank team at NCBI for productive discussion about their viral
609 genome submission requirements and facilitation of annotated genome deposition.
610
611 **Author Contributions**
612 M.J.T. conceived, performed, and validated experiments, developed methodologies and software,
613 performed analysis, curated data, wrote and revised the manuscript, and visualized data. D.V.P., N.L.W.,
614 B.S., A.P., and Y.S.P conceived and performed experiments and revised the manuscript. G.J.S. and S.R.K.
615 developed software and revised the manuscript. A.M.S. performed analysis, conceived of experiments,
616 and revised the manuscript. A.V. performed analysis, visualized data, and revised the manuscript. P.A.P.,
617 D.H.M., P.M.M., J.L.W., B.M., J.M.B., S.P.R., B.R., J.D., B.A.T., O.P., J.T., and S.M.R. provided resources
618 and reviewed the manuscript. B.B. and M.B.S. developed methods and software and reviewed the
619 manuscript. C.B.B. conceived of experiments, developed methods and software, supervised and
620 administered the project, and revised the manuscript.
621
622 **Declaration of Interests**
623 The authors declare no competing interests.
624
625 **Figure Legends**
626 Figure 1: Novel viruses associated with animal samples
627 Gross characterization of viruses discovered in this project compared to NCBI RefSeq virus database
628 entries. (A) Pie chart representing the number of viral genomes in broad categories. (B) Bar graph
629 showing the number of new representatives of known viral families or unclassified groups. Note that
630 genomes in this study were assigned taxonomy based on at least one region with a BLASTX hit with an E
631 value $<1\times10^{-5}$, suggesting commonality with a known viral family. Some genomes may ultimately be
632 characterized as being basal to the assigned family.
633

634 Figure 2: Sequence similarity network analysis of CRESS virus capsid proteins
635 EFI-EST was used to conduct pairwise alignments of amino acid sequences from this study and GenBank
636 with predicted structural similarity to CRESS virus capsid proteins. The E value cutoff for the analysis was
637 10^{-5}. (A) Cluster consisting of proteins with predicted structural similarity to geminivirus-like capsids
638 and/or STNV-like capsids. The phylogenetic tree was made from all sequences in this cluster. (B) A
639 cluster consisting of sequences with predicted structural similarity to Circovirus capsid proteins. The
640 phylogenetic tree was made from all sequences in this cluster. (C) Assorted clusters and singletons from
641 unclassified CRESS virus proteins that were modelled to be capsids. (D) Nanovirus capsids. (E) Gyrovirus
642 capsids.
643
644 Figure 3: Network analysis of CRESS virus Rep proteins
645 EFI-EST was used to conduct pairwise alignments of amino acid sequences from this study and
646 GenBank that were structurally modelled to be a rolling-circle replicase (Rep). The analysis used an E
647 value cutoff of 10^{-60} to divide the data into family-level clusters.
648
649 Figure 4: Genome maps of large CRESS virus genomes
650 Predicted CRESS Rep-like genes are displayed in orange, virion structural genes shown in green, other
651 identifiable viral genes shown in pink, other genes in grey. GenBank accession numbers are displayed
652 above the virus name.
653
654 Figure 5: RNA virus capsid-like proteins
655 Sequence similarity network generated with EFI-EST (E value cutoff of 10^{-5}) showing capsid protein
656 sequences of select ssRNA viruses (*Nodaviridae*, *Tombusviridae*, tombus-like viruses) and ssDNA viruses
657 (*Bacilladnaviridae* and crucivirus) together with protein sequences from DNA virus genomes observed in
658 the present study with predicted structural similarity to an RNA virus capsid protein domain (PDB:
659 2IZW). Predicted capsid proteins for CRESS virus ctca5 and CRESS virus ctgh4 have no detectible
660 similarity to any known DNA virus sequences. On the left, a phylogenetic tree representing the large
661 cluster is displayed. Collapsed branches consist of *Tombusviridae*, tombus-like viruses, and *Nodaviridae*
662 capsid genes.
663
664 Figure 6: Dark matter analysis
665 (A) Sequence similarity network analysis for genes from dark matter circular sequences (minimum
666 cluster size = 4). Clusters are colored based on assigned dark matter genome group (DMGG). Structural
667 predictions from HHpred are indicated (>85% probability). *Rep* = rolling circle replicases typical of CRESS
668 viruses or ssDNA plasmids. *Capsid* = single-jellyroll capsid protein. *Attachment* = cell attachment proteins
669 typical of inoviruses. *DNA-Binding* = DNA-binding domain. *PLA2* = phospholipase A2. *FtsL* = FtsL-like cell
670 division protein. Clusters that contain a representative protein that was successfully expressed as a
671 virus-like particle are outlined by a dashed rectangle (See Fig. 7). (B) Maps of three examples of DMGG1
672 with DMPCs labeled (linearized for display). (C) DMGG1 iVireons 'structure' score summary by protein
673 cluster. Scores range from -1 (unlikely to be a virion structural protein) to 1 (likely to be a virion
674 structural protein). Additional iVireons score summaries can be found in Fig. S8.
675
676 Figure 7: Expression of putative capsid proteins
677 Images taken by negative stain electron microscopy. Genome maps are linearized for display purposes.
678 Expressed genes are colored green. iVireons scores are listed in parentheses. (A-C) Images represent
679 virus-like particles from iVireons-predicted viral structural genes. (D) Merkel cell polyomavirus small T
680 antigen (a viral non-structural protein) is shown as a negative control.
681

682 Supplemental Figure 1: Divergence of proteins encoded by circular contigs
683 BLASTX summary of each circular DNA molecule recovered from virus enriched samples. Sequences
684 were queried against a database of viral and plasmid sequences. Only hits with E values < 10^{-5} were
685 plotted. Here, BLASTX only reports the most significant stretch of amino acid sequence from each
686 circular contig, and, therefore, other regions of each contig can be assumed to be equally or less
687 conserved.
688
689 Supplemental Figure 2: Size distribution of circular DNA sequences from this study
690 Length, in nucleotides, of circular DNA sequences representing putative viral genomes from this study.
691
692 Supplemental Figure 3: Network Analysis of additional viral hallmark genes
693 Depiction of additional viral hallmark genes from this study and GenBank as sequence similarity
694 networks. E value cutoff = 10^{-5}. See Figure 2 and Methods.
695
696 Supplemental Figure 4: Phylogenetic trees of viral hallmark genes
697 Sequences were aligned with PROMALS3D using structure guidance when possible. Trees were drawn
698 using IQ-Tree with automatic determination of substitution model. See methods. Branches are labeled
699 with bootstrap percent support after 1000 ultrafast bootstrapping events.
700 (A) *Microviridae* major capsid protein. (B) *Inoviridae* zonular occludens toxin. (C) CRESS virus Rep. (D)
701 *Anelloviridae* ORF1 (E) *Microviridae*/*Inoviridae* Replication-associated protein I. (F)
702 *Microviridae*/*Inoviridae* Replication-associated protein II. (G) *Microviridae*/*Inoviridae* Replication-
703 associated protein III.
704
705 Supplemental Figure 5: Nematode-associated virus capsid expression
706 Putative capsid proteins from CRESS virus ctdh33 associated with rhabditid nematodes (see Fig. 3) were
707 expressed in a human cell line. (A) Negative Stain EM images of virus-like particles resulting from the
708 expression of all three genes predicted to encode STNV-like capsid proteins. (B) Agarose gel
709 electrophoretic analysis of nucleic acids extracted from ctdh33 VLPs shows that purified VLPs from
710 fraction 4 of the Optiprep gradient contain encapsidated RNA. Note that Benzonase digests both DNA
711 and RNA, DnaseI only digests DNA and Rnase only digests RNA.
712
713 Supplemental Figure 6: Genome maps of additional CRESS genomes encoding multiple capsid genes
714 CRESS Rep genes are shown in orange, predicted virion structural genes in green, other candidate genes
715 in gray.
716
717 Supplemental Figure 7: Validation of proteins with predicted similarity to RNA virus capsid proteins
718 (A) First order neighbors for Crucian-associated CRESS virus ctgh4 capsid protein were extracted from
719 the network shown in Figure 5 and aligned using Muscle. (B) The same approach was applied to CRESS
720 virus ctbd466 capsid protein. (C) A visualization (Integrative Genomics Viewer) of a read alignment to
721 CRESS virus isolate ctca5. The visualization shows no evidence of artifactual chimerization in the contig
722 assembly process.
723
724 Supplementary Figure 8 (related to Figure 6): iVireons scores of DMGGs with candidate viral structural
725 gene(s)
726 Box-and-whisker plots of iVireons 'Structural' scores for individual DMPCs (numbers on x-axes) grouped
727 by DMGG. Scores (y-axes) range from -1 (unlikely to be a virion structural protein) to 1 (likely to be a
728 virion structural protein). DMGG2 and DMGG3 have been combined due to inferred chimerism.
729

730 Supplemental Figure 9: Sample characterization by iterative BLAST Searches
731 Contigs of over 1000 nts from each sample were subject to iterative BLAST searches. First, BLASTN was
732 performed against the RefSeq database. Contigs without hits were then queried by BLASTX against all of
733 GenBank 'nr' database. Contigs without hits were then queried by BLASTX against a database of proteins
734 from genomes reported in this study. The proportion of total reads mapping to each contig was
735 calculated and used for this plot. Individual inspection of contigs shows that most hits in the 'Translated
736 AA alignment to GenBank 'nr' "Bacteria"' were likely plasmid or prophage proteins. The proportions of
737 hits in each category are sensitive to stringency settings and to which databases are chosen for the
738 analysis. The key aims of the figure are to display the proportion of reads the current survey rendered
739 classifiable and the fraction of remaining dark matter reads in various samples.
740
741 **References**
742

743 AGRANOVSKY, A. A., LESEMANN, D. E., MAISS, E., HULL, R. & ATABEKOV, J. G. 1995.
744 "Rattlesnake" structure of a filamentous plant RNA virus built of two capsid proteins.
745 *Proc Natl Acad Sci U S A,* 92**,** 2470-3.
746 ALTSCHUL, S. F., GISH, W., MILLER, W., MYERS, E. W. & LIPMAN, D. J. 1990. Basic local
747 alignment search tool. *J Mol Biol,* 215**,** 403-10.
748 ASPLUND, M., KJARTANSDOTTIR, K. R., MOLLERUP, S., VINNER, L., FRIDHOLM, H.,
749 HERRERA, J. A. R., FRIIS-NIELSEN, J., HANSEN, T. A., JENSEN, R. H., NIELSEN, I.
750 B., RICHTER, S. R., REY-IGLESIA, A., MATEY-HERNANDEZ, M. L., ALQUEZAR-
751 PLANAS, D. E., OLSEN, P. V. S., SICHERITZ-PONTEN, T., WILLERSLEV, E., LUND,
752 O., BRUNAK, S., MOURIER, T., NIELSEN, L. P., IZARZUGAZA, J. M. G. & HANSEN,
753 A. J. 2019. Contaminating viral sequences in high-throughput sequencing viromics: a
754 linkage study of 700 sequencing libraries. *Clin Microbiol Infect*.
755 BEDELL, M. A., HUDSON, J. B., GOLUB, T. R., TURYK, M. E., HOSKEN, M., WILBANKS, G.
756 D. & LAIMINS, L. A. 1991. Amplification of human papillomavirus genomes in vitro is
757 dependent on epithelial differentiation. *J Virol,* 65**,** 2254-60.
758 BIN JANG, H., BOLDUC, B., ZABLOCKI, O., KUHN, J. H., ROUX, S., ADRIAENSSENS, E. M.,
759 BRISTER, J. R., KROPINSKI, A. M., KRUPOVIC, M., LAVIGNE, R., TURNER, D. &
760 SULLIVAN, M. B. 2019. Taxonomic assignment of uncultivated prokaryotic virus
761 genomes is enabled by gene-sharing networks. *Nat Biotechnol,* 37**,** 632-639.
762 BLINKOVA, O., VICTORIA, J., LI, Y., KEELE, B. F., SANZ, C., NDJANGO, J. B., PEETERS, M.,
763 TRAVIS, D., LONSDORF, E. V., WILSON, M. L., PUSEY, A. E., HAHN, B. H. &
764 DELWART, E. L. 2010. Novel circular DNA viruses in stool samples of wild-living
765 chimpanzees. *J Gen Virol,* 91**,** 74-86.
766 BOLDUC, B., JANG, H. B., DOULCIER, G., YOU, Z. Q., ROUX, S. & SULLIVAN, M. B. 2017.
767 vConTACT: an iVirus tool to classify double-stranded DNA viruses that infect Archaea
768 and Bacteria. *PeerJ,* 5**,** e3243.
769 BOTTCHER, B., UNSELD, S., CEULEMANS, H., RUSSELL, R. B. & JESKE, H. 2004.
770 Geminate structures of African cassava mosaic virus. *J Virol,* 78**,** 6758-65.
771 BRISTER, J. R., AKO-ADJEI, D., BAO, Y. & BLINKOVA, O. 2015. NCBI viral genomes
772 resource. *Nucleic Acids Res,* 43**,** D571-7.
773 BUCK, C. B., PASTRANA, D. V., LOWY, D. R. & SCHILLER, J. T. 2004. Efficient intracellular
774 assembly of papillomaviral vectors. *J Virol,* 78**,** 751-7.
775 BUCK, C. B., VAN DOORSLAER, K., PERETTI, A., GEOGHEGAN, E. M., TISZA, M. J., AN, P.,
776 KATZ, J. P., PIPAS, J. M., MCBRIDE, A. A., CAMUS, A. C., MCDERMOTT, A. J., DILL,
777 J. A., DELWART, E., NG, T. F., FARKAS, K., AUSTIN, C., KRABERGER, S., DAVISON,
778 W., PASTRANA, D. V. & VARSANI, A. 2016. The Ancient Evolutionary History of
779 Polyomaviruses. *PLoS Pathog,* 12**,** e1005574.

780 BURLEY, S. K., BERMAN, H. M., KLEYWEGT, G. J., MARKLEY, J. L., NAKAMURA, H. &
781 VELANKAR, S. 2017. Protein Data Bank (PDB): The Single Global Macromolecular
782 Structure Archive. *Methods Mol Biol,* 1607**,** 627-641.
783 CHALKIAS, S., GORHAM, J. M., MAZAIKA, E., PARFENOV, M., DANG, X., DEPALMA, S.,
784 MCKEAN, D., SEIDMAN, C. E., SEIDMAN, J. G. & KORALNIK, I. J. 2018. ViroFind: A
785 novel target-enrichment deep-sequencing platform reveals a complex JC virus
786 population in the brain of PML patients. *PLoS One,* 13**,** e0186945.
787 CHANDONIA, J. M., FOX, N. K. & BRENNER, S. E. 2019. SCOPe: classification of large
788 macromolecular structures in the structural classification of proteins-extended database.
789 *Nucleic Acids Res,* 47**,** D475-D481.
790 CHEN, J., TSAI, V., PARKER, W. E., ARONICA, E., BAYBIS, M. & CRINO, P. B. 2012.
791 Detection of human papillomavirus in human focal cortical dysplasia type IIB. *Ann*
792 *Neurol,* 72**,** 881-92.
793 CORAS, R., KORN, K., BIEN, C. G., KALBHENN, T., ROSSLER, K., KOBOW, K., GIEDL, J.,
794 FLECKENSTEIN, B. & BLUMCKE, I. 2015. No evidence for human papillomavirus
795 infection in focal cortical dysplasia IIb. *Ann Neurol,* 77**,** 312-9.
796 DAYARAM, A., GALATOWITSCH, M. L., ARGUELLO-ASTORGA, G. R., VAN BYSTERVELDT,
797 K., KRABERGER, S., STAINTON, D., HARDING, J. S., ROUMAGNAC, P., MARTIN, D.
798 P., LEFEUVRE, P. & VARSANI, A. 2016. Diverse circular replication-associated protein
799 encoding viruses circulating in invertebrates within a lake ecosystem. *Infect Genet Evol,*
800 39**,** 304-316.
801 DAYARAM, A., GOLDSTIEN, S., ARGUELLO-ASTORGA, G. R., ZAWAR-REZA, P., GOMEZ,
802 C., HARDING, J. S. & VARSANI, A. 2015. Diverse small circular DNA viruses circulating
803 amongst estuarine molluscs. *Infect Genet Evol,* 31**,** 284-95.
804 DÍEZ-VILLASEÑOR, C. & RODRIGUEZ-VALERA, F. 2019. CRISPR analysis suggests that
805 small circular single-stranded DNA smacoviruses infect Archaea instead of humans.
806 *Nature Communications,* 10**,** 294.
807 EIMER, W. A., VIJAYA KUMAR, D. K., NAVALPUR SHANMUGAM, N. K., RODRIGUEZ, A. S.,
808 MITCHELL, T., WASHICOSKY, K. J., GYORGY, B., BREAKEFIELD, X. O., TANZI, R. E.
809 & MOIR, R. D. 2018. Alzheimer's Disease-Associated beta-Amyloid Is Rapidly Seeded
810 by Herpesviridae to Protect against Brain Infection. *Neuron,* 99**,** 56-63 e3.
811 EL-GEBALI, S., MISTRY, J., BATEMAN, A., EDDY, S. R., LUCIANI, A., POTTER, S. C.,
812 QURESHI, M., RICHARDSON, L. J., SALAZAR, G. A., SMART, A., SONNHAMMER, E.
813 L. L., HIRSH, L., PALADIN, L., PIOVESAN, D., TOSATTO, S. C. E. & FINN, R. D. 2019.
814 The Pfam protein families database in 2019. *Nucleic Acids Res,* 47**,** D427-D432.
815 EMERSON, J. B., ROUX, S., BRUM, J. R., BOLDUC, B., WOODCROFT, B. J., JANG, H. B.,
816 SINGLETON, C. M., SOLDEN, L. M., NAAS, A. E., BOYD, J. A., HODGKINS, S. B.,
817 WILSON, R. M., TRUBL, G., LI, C., FROLKING, S., POPE, P. B., WRIGHTON, K. C.,
818 CRILL, P. M., CHANTON, J. P., SALESKA, S. R., TYSON, G. W., RICH, V. I. &
819 SULLIVAN, M. B. 2018. Host-linked soil viral ecology along a permafrost thaw gradient.
820 *Nat Microbiol,* 3**,** 870-880.
821 FALERO, A., CABALLERO, A., FERRAN, B., IZQUIERDO, Y., FANDO, R. & CAMPOS, J.
822 2009. DNA binding proteins of the filamentous phages CTXphi and VGJphi of Vibrio
823 cholerae. *J Bacteriol,* 191**,** 5873-6.
824 FONTENELE, R. S., LACORTE, C., LAMAS, N. S., SCHMIDLIN, K., VARSANI, A. & RIBEIRO,
825 S. G. 2019. Single Stranded DNA Viruses Associated with Capybara Faeces Sampled in
826 Brazil. *Viruses,* 11.
827 FU, L., NIU, B., ZHU, Z., WU, S. & LI, W. 2012. CD-HIT: accelerated for clustering the next-
828 generation sequencing data. *Bioinformatics,* 28**,** 3150-2.
829 GEOGHEGAN, E. M., PASTRANA, D. V., SCHOWALTER, R. M., RAY, U., GAO, W., HO, M.,
830 PAULY, G. T., SIGANO, D. M., KAYNOR, C., CAHIR-MCFARLAND, E.,

831 COMBALUZIER, B., GRIMM, J. & BUCK, C. B. 2017. Infectious Entry and Neutralization
832 of Pathogenic JC Polyomaviruses. *Cell Rep,* 21**,** 1169-1179.
833 GERLT, J. A., BOUVIER, J. T., DAVIDSON, D. B., IMKER, H. J., SADKHIN, B., SLATER, D. R.
834 & WHALEN, K. L. 2015. Enzyme Function Initiative-Enzyme Similarity Tool (EFI-EST): A
835 web tool for generating protein sequence similarity networks. *Biochim Biophys Acta,*
836 1854**,** 1019-37.
837 GILBERT, J. A., MEYER, F., ANTONOPOULOS, D., BALAJI, P., BROWN, C. T., BROWN, C.
838 T., DESAI, N., EISEN, J. A., EVERS, D., FIELD, D., FENG, W., HUSON, D., JANSSON,
839 J., KNIGHT, R., KNIGHT, J., KOLKER, E., KONSTANTINDIS, K., KOSTKA, J.,
840 KYRPIDES, N., MACKELPRANG, R., MCHARDY, A., QUINCE, C., RAES, J.,
841 SCZYRBA, A., SHADE, A. & STEVENS, R. 2010. Meeting report: the terabase
842 metagenomics workshop and the vision of an Earth microbiome project. *Stand Genomic*
843 *Sci,* 3**,** 243-8.
844 GREGORY, A. C., ZAYED, A. A., CONCEICAO-NETO, N., TEMPERTON, B., BOLDUC, B.,
845 ALBERTI, A., ARDYNA, M., ARKHIPOVA, K., CARMICHAEL, M., CRUAUD, C.,
846 DIMIER, C., DOMINGUEZ-HUERTA, G., FERLAND, J., KANDELS, S., LIU, Y., MAREC,
847 C., PESANT, S., PICHERAL, M., PISAREV, S., POULAIN, J., TREMBLAY, J. E., VIK,
848 D., TARA OCEANS, C., BABIN, M., BOWLER, C., CULLEY, A. I., DE VARGAS, C.,
849 DUTILH, B. E., IUDICONE, D., KARP-BOSS, L., ROUX, S., SUNAGAWA, S.,
850 WINCKER, P. & SULLIVAN, M. B. 2019. Marine DNA Viral Macro- and Microdiversity
851 from Pole to Pole. *Cell,* 177**,** 1109-1123 e14.
852 GRENINGER, A. L. & DERISI, J. L. 2015. Draft Genome Sequences of Ciliovirus and Brinovirus
853 from San Francisco Wastewater. *Genome Announc,* 3.
854 GROSE, J. H. & CASJENS, S. R. 2014. Understanding the enormous diversity of
855 bacteriophages: the tailed phages that infect the bacterial family Enterobacteriaceae.
856 *Virology,* 468-470**,** 421-443.
857 GROSE, J. H., JENSEN, G. L., BURNETT, S. H. & BREAKWELL, D. P. 2014. Genomic
858 comparison of 93 Bacillus phages reveals 12 clusters, 14 singletons and remarkable
859 diversity. *BMC Genomics,* 15**,** 855.
860 HIPP, K., GRIMM, C., JESKE, H. & BOTTCHER, B. 2017. Near-Atomic Resolution Structure of
861 a Plant Geminivirus Determined by Electron Cryomicroscopy. *Structure,* 25**,** 1303-1309
862 e3.
863 HODYRA-STEFANIAK, K., MIERNIKIEWICZ, P., DRAPALA, J., DRAB, M., JONCZYK-
864 MATYSIAK, E., LECION, D., KAZMIERCZAK, Z., BETA, W., MAJEWSKA, J.,
865 HARHALA, M., BUBAK, B., KLOPOT, A., GORSKI, A. & DABROWSKA, K. 2015.
866 Mammalian Host-Versus-Phage immune response determines phage fate in vivo. *Sci*
867 *Rep,* 5**,** 14802.
868 HUANG, Y. J., MAO, B., ARAMINI, J. M. & MONTELIONE, G. T. 2014. Assessment of
869 template-based protein structure predictions in CASP10. *Proteins,* 82 Suppl 2**,** 43-56.
870 HUNT, M., SILVA, N. D., OTTO, T. D., PARKHILL, J., KEANE, J. A. & HARRIS, S. R. 2015.
871 Circlator: automated circularization of genome assemblies using long sequencing reads.
872 *Genome Biol,* 16**,** 294.
873 IRANZO, J., KRUPOVIC, M. & KOONIN, E. V. 2017. A network perspective on the virus world.
874 *Commun Integr Biol,* 10**,** e1296614.
875 ITZHAKI, R. F., LATHE, R., BALIN, B. J., BALL, M. J., BEARER, E. L., BRAAK, H., BULLIDO,
876 M. J., CARTER, C., CLERICI, M., COSBY, S. L., DEL TREDICI, K., FIELD, H., FULOP,
877 T., GRASSI, C., GRIFFIN, W. S., HAAS, J., HUDSON, A. P., KAMER, A. R., KELL, D.
878 B., LICASTRO, F., LETENNEUR, L., LOVHEIM, H., MANCUSO, R., MIKLOSSY, J.,
879 OTTH, C., PALAMARA, A. T., PERRY, G., PRESTON, C., PRETORIUS, E.,
880 STRANDBERG, T., TABET, N., TAYLOR-ROBINSON, S. D. & WHITTUM-HUDSON, J.
881 A. 2016. Microbes and Alzheimer's Disease. *J Alzheimers Dis,* 51**,** 979-84.

882 KATOH, K. & STANDLEY, D. M. 2013. MAFFT multiple sequence alignment software version 7:
883 improvements in performance and usability. *Mol Biol Evol,* 30**,** 772-80.
884 KAUFFMAN, K. M., HUSSAIN, F. A., YANG, J., AREVALO, P., BROWN, J. M., CHANG, W. K.,
885 VANINSBERGHE, D., ELSHERBINI, J., SHARMA, R. S., CUTLER, M. B., KELLY, L. &
886 POLZ, M. F. 2018. A major lineage of non-tailed dsDNA viruses as unrecognized killers
887 of marine bacteria. *Nature,* 554**,** 118-122.
888 KAZLAUSKAS, D., DAYARAM, A., KRABERGER, S., GOLDSTIEN, S., VARSANI, A. &
889 KRUPOVIC, M. 2017. Evolutionary history of ssDNA bacilladnaviruses features
890 horizontal acquisition of the capsid gene from ssRNA nodaviruses. *Virology,* 504**,** 114-
891 121.
892 KAZLAUSKAS, D., VARSANI, A., KOONIN, E. V. & KRUPOVIC, M. 2019. Multiple origins of
893 prokaryotic and eukaryotic single-stranded DNA viruses from bacterial and archaeal
894 plasmids. *Nat Commun,* 10**,** 3425.
895 KELLEY, L. A., MEZULIS, S., YATES, C. M., WASS, M. N. & STERNBERG, M. J. 2015. The
896 Phyre2 web portal for protein modeling, prediction and analysis. *Nat Protoc,* 10**,** 845-58.
897 KHAYAT, R., BRUNN, N., SPEIR, J. A., HARDHAM, J. M., ANKENBAUER, R. G.,
898 SCHNEEMANN, A. & JOHNSON, J. E. 2011. The 2.3-angstrom structure of porcine
899 circovirus 2. *J Virol,* 85**,** 7856-62.
900 KIM, K. H., CHANG, H. W., NAM, Y. D., ROH, S. W., KIM, M. S., SUNG, Y., JEON, C. O., OH,
901 H. M. & BAE, J. W. 2008. Amplification of uncultured single-stranded DNA viruses from
902 rice paddy soil. *Appl Environ Microbiol,* 74**,** 5975-85.
903 KING, A. M. Q., LEFKOWITZ, E. J., MUSHEGIAN, A. R., ADAMS, M. J., DUTILH, B. E.,
904 GORBALENYA, A. E., HARRACH, B., HARRISON, R. L., JUNGLEN, S., KNOWLES, N.
905 J., KROPINSKI, A. M., KRUPOVIC, M., KUHN, J. H., NIBERT, M. L., RUBINO, L.,
906 SABANADZOVIC, S., SANFACON, H., SIDDELL, S. G., SIMMONDS, P., VARSANI, A.,
907 ZERBINI, F. M. & DAVISON, A. J. 2018. Changes to taxonomy and the International
908 Code of Virus Classification and Nomenclature ratified by the International Committee on
909 Taxonomy of Viruses (2018). *Arch Virol*.
910 KOONIN, E. V., DOLJA, V. V. & KRUPOVIC, M. 2015. Origins and evolution of viruses of
911 eukaryotes: The ultimate modularity. *Virology,* 479-480**,** 2-25.
912 KRABERGER, S., ARGUELLO-ASTORGA, G. R., GREENFIELD, L. G., GALILEE, C., LAW, D.,
913 MARTIN, D. P. & VARSANI, A. 2015. Characterisation of a diverse range of circular
914 replication-associated protein encoding DNA viruses recovered from a sewage treatment
915 oxidation pond. *Infect Genet Evol,* 31**,** 73-86.
916 KRABERGER, S., SCHMIDLIN, K., FONTENELE, R. S., WALTERS, M. & VARSANI, A. 2019.
917 Unravelling the Single-Stranded DNA Virome of the New Zealand Blackfly. *Viruses,* 11.
918 KRISHNAMURTHY, S. R. & WANG, D. 2017. Origins and challenges of viral dark matter. *Virus*
919 *Res,* 239**,** 136-142.
920 KRUPOVIC, M., GHABRIAL, S. A., JIANG, D. & VARSANI, A. 2016. Genomoviridae: a new
921 family of widespread single-stranded DNA viruses. *Arch Virol,* 161**,** 2633-43.
922 KRUPOVIC, M. & KOONIN, E. V. 2017. Multiple origins of viral capsid proteins from cellular
923 ancestors. *Proc Natl Acad Sci U S A,* 114**,** E2401-E2410.
924 KRUPOVIC, M., RAVANTTI, J. J. & BAMFORD, D. H. 2009. Geminiviruses: a tale of a plasmid
925 becoming a virus. *BMC Evol Biol,* 9**,** 112.
926 KRUPOVIC, M., ZHI, N., LI, J., HU, G., KOONIN, E. V., WONG, S., SHEVCHENKO, S., ZHAO,
927 K. & YOUNG, N. S. 2015. Multiple layers of chimerism in a single-stranded DNA virus
928 discovered by deep sequencing. *Genome Biol Evol,* 7**,** 993-1001.
929 LABONTE, J. M. & SUTTLE, C. A. 2013. Previously unknown and highly divergent ssDNA
930 viruses populate the oceans. *ISME J,* 7**,** 2169-77.
931 LEFEUVRE, P., MARTIN, D. P., ELENA, S. F., SHEPHERD, D. N., ROUMAGNAC, P. &
932 VARSANI, A. 2019. Evolution and ecology of plant viruses. *Nat Rev Microbiol*.

933 LETUNIC, I. & BORK, P. 2019. Interactive Tree Of Life (iTOL) v4: recent updates and new
934 developments. *Nucleic Acids Res,* 47**,** W256-W259.
935 LIMA-MENDEZ, G., VAN HELDEN, J., TOUSSAINT, A. & LEPLAE, R. 2008. Reticulate
936 representation of evolutionary and functional relationships between phage genomes. *Mol*
937 *Biol Evol,* 25**,** 762-77.
938 LLOYD-PRICE, J., MAHURKAR, A., RAHNAVARD, G., CRABTREE, J., ORVIS, J., HALL, A.
939 B., BRADY, A., CREASY, H. H., MCCRACKEN, C., GIGLIO, M. G., MCDONALD, D.,
940 FRANZOSA, E. A., KNIGHT, R., WHITE, O. & HUTTENHOWER, C. 2017. Strains,
941 functions and dynamics in the expanded Human Microbiome Project. *Nature,* 550**,** 61-
942 66.
943 MAKINO, D. L., LARSON, S. B. & MCPHERSON, A. 2013. The crystallographic structure of
944 Panicum Mosaic Virus (PMV). *J Struct Biol,* 181**,** 37-52.
945 MARCHLER-BAUER, A. & BRYANT, S. H. 2004. CD-Search: protein domain annotations on
946 the fly. *Nucleic Acids Res,* 32**,** W327-31.
947 MARCHLER-BAUER, A., DERBYSHIRE, M. K., GONZALES, N. R., LU, S., CHITSAZ, F.,
948 GEER, L. Y., GEER, R. C., HE, J., GWADZ, M., HURWITZ, D. I., LANCZYCKI, C. J.,
949 LU, F., MARCHLER, G. H., SONG, J. S., THANKI, N., WANG, Z., YAMASHITA, R. A.,
950 ZHANG, D., ZHENG, C. & BRYANT, S. H. 2015. CDD: NCBI's conserved domain
951 database. *Nucleic Acids Res,* 43**,** D222-6.
952 MEIER, A. & SODING, J. 2015. Automatic Prediction of Protein 3D Structures by Probabilistic
953 Multi-template Homology Modeling. *PLoS Comput Biol,* 11**,** e1004343.
954 NGUYEN, L. T., SCHMIDT, H. A., VON HAESELER, A. & MINH, B. Q. 2015. IQ-TREE: a fast
955 and effective stochastic algorithm for estimating maximum-likelihood phylogenies. *Mol*
956 *Biol Evol,* 32**,** 268-74.
957 O'LEARY, N. A., WRIGHT, M. W., BRISTER, J. R., CIUFO, S., HADDAD, D., MCVEIGH, R.,
958 RAJPUT, B., ROBBERTSE, B., SMITH-WHITE, B., AKO-ADJEI, D., ASTASHYN, A.,
959 BADRETDIN, A., BAO, Y., BLINKOVA, O., BROVER, V., CHETVERNIN, V., CHOI, J.,
960 COX, E., ERMOLAEVA, O., FARRELL, C. M., GOLDFARB, T., GUPTA, T., HAFT, D.,
961 HATCHER, E., HLAVINA, W., JOARDAR, V. S., KODALI, V. K., LI, W., MAGLOTT, D.,
962 MASTERSON, P., MCGARVEY, K. M., MURPHY, M. R., O'NEILL, K., PUJAR, S.,
963 RANGWALA, S. H., RAUSCH, D., RIDDICK, L. D., SCHOCH, C., SHKEDA, A., STORZ,
964 S. S., SUN, H., THIBAUD-NISSEN, F., TOLSTOY, I., TULLY, R. E., VATSAN, A. R.,
965 WALLIN, C., WEBB, D., WU, W., LANDRUM, M. J., KIMCHI, A., TATUSOVA, T.,
966 DICUCCIO, M., KITTS, P., MURPHY, T. D. & PRUITT, K. D. 2016. Reference sequence
967 (RefSeq) database at NCBI: current status, taxonomic expansion, and functional
968 annotation. *Nucleic Acids Res,* 44**,** D733-45.
969 OH, J., BYRD, A. L., DEMING, C., CONLAN, S., KONG, H. H., SEGRE, J. A. & PROGRAM, N.
970 C. S. 2014. Biogeography and individuality shape function in the human skin
971 metagenome. *Nature,* 514**,** 59-64.
972 PAEZ-ESPINO, D., ELOE-FADROSH, E. A., PAVLOPOULOS, G. A., THOMAS, A. D.,
973 HUNTEMANN, M., MIKHAILOVA, N., RUBIN, E., IVANOVA, N. N. & KYRPIDES, N. C.
974 2016. Uncovering Earth's virome. *Nature,* 536**,** 425-30.
975 PAEZ-ESPINO, D., ROUX, S., CHEN, I. A., PALANIAPPAN, K., RATNER, A., CHU, K.,
976 HUNTEMANN, M., REDDY, T. B. K., PONS, J. C., LLABRES, M., ELOE-FADROSH, E.
977 A., IVANOVA, N. N. & KYRPIDES, N. C. 2019. IMG/VR v.2.0: an integrated data
978 management and analysis system for cultivated and environmental viral genomes.
979 *Nucleic Acids Res,* 47**,** D678-D686.
980 PASTRANA, D. V., PERETTI, A., WELCH, N. L., BORGOGNA, C., OLIVERO, C., BADOLATO,
981 R., NOTARANGELO, L. D., GARIGLIO, M., FITZGERALD, P. C., MCINTOSH, C. E.,
982 REEVES, J., STARRETT, G. J., BLISKOVSKY, V., VELEZ, D., BROWNELL, I.,
983 YARCHOAN, R., WYVILL, K. M., ULDRICK, T. S., MALDARELLI, F., LISCO, A.,

984 SERETI, I., GONZALEZ, C. M., ANDROPHY, E. J., MCBRIDE, A. A., VAN
985 DOORSLAER, K., GARCIA, F., DVORETZKY, I., LIU, J. S., HAN, J., MURPHY, P. M.,
986 MCDERMOTT, D. H. & BUCK, C. B. 2018. Metagenomic Discovery of 83 New Human
987 Papillomavirus Types in Patients with Immunodeficiency. *mSphere,* 3.
988 PEI, J. & GRISHIN, N. V. 2014. PROMALS3D: multiple protein sequence alignment enhanced
989 with evolutionary and three-dimensional structural information. *Methods Mol Biol,* 1079**,**
990 263-71.
991 PERETTI, A., FITZGERALD, P. C., BLISKOVSKY, V., BUCK, C. B. & PASTRANA, D. V. 2015.
992 Hamburger polyomaviruses. *J Gen Virol,* 96**,** 833-9.
993 POPE, W. H., BOWMAN, C. A., RUSSELL, D. A., JACOBS-SERA, D., ASAI, D. J., CRESAWN,
994 S. G., JACOBS, W. R., HENDRIX, R. W., LAWRENCE, J. G., HATFULL, G. F.,
995 SCIENCE EDUCATION ALLIANCE PHAGE HUNTERS ADVANCING, G.,
996 EVOLUTIONARY, S., PHAGE HUNTERS INTEGRATING, R., EDUCATION &
997 MYCOBACTERIAL GENETICS, C. 2015. Whole genome comparison of a large
998 collection of mycobacteriophages reveals a continuum of phage genetic diversity. *Elife,*
999 4**,** e06416.
1000 QUAISER, A., KRUPOVIC, M., DUFRESNE, A., FRANCEZ, A. J. & ROUX, S. 2016. Diversity
1001 and comparative genomics of chimeric viruses in Sphagnum-dominated peatlands. *Virus*
1002 *Evol,* 2**,** vew025.
1003 REMMERT, M., BIEGERT, A., HAUSER, A. & SÖDING, J. 2011. HHblits: lightning-fast iterative
1004 protein sequence searching by HMM-HMM alignment. *Nat Methods,* 9**,** 173-5.
1005 ROHWER, F. & EDWARDS, R. 2002. The Phage Proteomic Tree: a genome-based taxonomy
1006 for phage. *J Bacteriol,* 184**,** 4529-35.
1007 ROSARIO, K., BREITBART, M., HARRACH, B., SEGALES, J., DELWART, E., BIAGINI, P. &
1008 VARSANI, A. 2017. Revisiting the taxonomy of the family Circoviridae: establishment of
1009 the genus Cyclovirus and removal of the genus Gyrovirus. *Arch Virol,* 162**,** 1447-1463.
1010 ROSARIO, K., METTEL, K. A., BENNER, B. E., JOHNSON, R., SCOTT, C., YUSSEFF-
1011 VANEGAS, S. Z., BAKER, C. C. M., CASSILL, D. L., STORER, C., VARSANI, A. &
1012 BREITBART, M. 2018. Virus discovery in all three major lineages of terrestrial
1013 arthropods highlights the diversity of single-stranded DNA viruses associated with
1014 invertebrates. *PeerJ,* 6**,** e5761.
1015 ROUX, S., ADRIAENSSENS, E. M., DUTILH, B. E., KOONIN, E. V., KROPINSKI, A. M.,
1016 KRUPOVIC, M., KUHN, J. H., LAVIGNE, R., BRISTER, J. R., VARSANI, A., AMID, C.,
1017 AZIZ, R. K., BORDENSTEIN, S. R., BORK, P., BREITBART, M., COCHRANE, G. R.,
1018 DALY, R. A., DESNUES, C., DUHAIME, M. B., EMERSON, J. B., ENAULT, F.,
1019 FUHRMAN, J. A., HINGAMP, P., HUGENHOLTZ, P., HURWITZ, B. L., IVANOVA, N. N.,
1020 LABONTE, J. M., LEE, K. B., MALMSTROM, R. R., MARTINEZ-GARCIA, M.,
1021 MIZRACHI, I. K., OGATA, H., PAEZ-ESPINO, D., PETIT, M. A., PUTONTI, C., RATTEI,
1022 T., REYES, A., RODRIGUEZ-VALERA, F., ROSARIO, K., SCHRIML, L., SCHULZ, F.,
1023 STEWARD, G. F., SULLIVAN, M. B., SUNAGAWA, S., SUTTLE, C. A., TEMPERTON,
1024 B., TRINGE, S. G., THURBER, R. V., WEBSTER, N. S., WHITESON, K. L., WILHELM,
1025 S. W., WOMMACK, K. E., WOYKE, T., WRIGHTON, K. C., YILMAZ, P., YOSHIDA, T.,
1026 YOUNG, M. J., YUTIN, N., ALLEN, L. Z., KYRPIDES, N. C. & ELOE-FADROSH, E. A.
1027 2019a. Minimum Information about an Uncultivated Virus Genome (MIUViG). *Nature*
1028 *Biotechnology,* 37**,** 29-37.
1029 ROUX, S., ENAULT, F., BRONNER, G., VAULOT, D., FORTERRE, P. & KRUPOVIC, M. 2013.
1030 Chimeric viruses blur the borders between the major groups of eukaryotic single-
1031 stranded DNA viruses. *Nat Commun,* 4**,** 2700.
1032 ROUX, S., ENAULT, F., HURWITZ, B. L. & SULLIVAN, M. B. 2015. VirSorter: mining viral
1033 signal from microbial genomic data. *PeerJ,* 3**,** e985.

1034 ROUX, S., KRUPOVIC, M., DALY, R. A., BORGES, A. L., NAYFACH, S., SCHULZ, F.,
1035 SHARRAR, A., MATHEUS CARNEVALI, P. B., CHENG, J. F., IVANOVA, N. N.,
1036 BONDY-DENOMY, J., WRIGHTON, K. C., WOYKE, T., VISEL, A., KYRPIDES, N. C. &
1037 ELOE-FADROSH, E. A. 2019b. Cryptic inoviruses revealed as pervasive in bacteria and
1038 archaea across Earth's biomes. *Nat Microbiol*.
1039 SCHULZ, F., YUTIN, N., IVANOVA, N. N., ORTEGA, D. R., LEE, T. K., VIERHEILIG, J.,
1040 DAIMS, H., HORN, M., WAGNER, M., JENSEN, G. J., KYRPIDES, N. C., KOONIN, E.
1041 V. & WOYKE, T. 2017. Giant viruses with an expanded complement of translation
1042 system components. *Science,* 356**,** 82-85.
1043 SEGURITAN, V., ALVES, N., JR., ARNOULT, M., RAYMOND, A., LORIMER, D., BURGIN, A.
1044 B., JR., SALAMON, P. & SEGALL, A. M. 2012. Artificial neural networks trained to
1045 detect viral and phage structural proteins. *PLoS Comput Biol,* 8**,** e1002657.
1046 SHI, M., LIN, X. D., TIAN, J. H., CHEN, L. J., CHEN, X., LI, C. X., QIN, X. C., LI, J., CAO, J. P.,
1047 EDEN, J. S., BUCHMANN, J., WANG, W., XU, J., HOLMES, E. C. & ZHANG, Y. Z.
1048 2016. Redefining the invertebrate RNA virosphere. *Nature*.
1049 SIMMONDS, P., ADAMS, M. J., BENKO, M., BREITBART, M., BRISTER, J. R., CARSTENS, E.
1050 B., DAVISON, A. J., DELWART, E., GORBALENYA, A. E., HARRACH, B., HULL, R.,
1051 KING, A. M., KOONIN, E. V., KRUPOVIC, M., KUHN, J. H., LEFKOWITZ, E. J.,
1052 NIBERT, M. L., ORTON, R., ROOSSINCK, M. J., SABANADZOVIC, S., SULLIVAN, M.
1053 B., SUTTLE, C. A., TESH, R. B., VAN DER VLUGT, R. A., VARSANI, A. & ZERBINI, F.
1054 M. 2017. Consensus statement: Virus taxonomy in the age of metagenomics. *Nat Rev*
1055 *Microbiol,* 15**,** 161-168.
1056 STEEL, O., KRABERGER, S., SIKORSKI, A., YOUNG, L. M., CATCHPOLE, R. J., STEVENS,
1057 A. J., LADLEY, J. J., CORAY, D. S., STAINTON, D., DAYARAM, A., JULIAN, L., VAN
1058 BYSTERVELDT, K. & VARSANI, A. 2016. Circular replication-associated protein
1059 encoding DNA viruses identified in the faecal matter of various animals in New Zealand.
1060 *Infect Genet Evol,* 43**,** 151-64.
1061 SU, G., MORRIS, J. H., DEMCHAK, B. & BADER, G. D. 2014. Biological network exploration
1062 with Cytoscape 3. *Curr Protoc Bioinformatics,* 47**,** 8.13.1-24.
1063 SULLIVAN, M. B. 2015. Viromes, not gene markers, for studying double-stranded DNA virus
1064 communities. *J Virol,* 89**,** 2459-61.
1065 TOMARU, Y., TAKAO, Y., SUZUKI, H., NAGUMO, T., KOIKE, K. & NAGASAKI, K. 2011.
1066 Isolation and characterization of a single-stranded DNA virus infecting Chaetoceros
1067 lorenzianus Grunow. *Appl Environ Microbiol,* 77**,** 5285-93.
1068 TURNBAUGH, P. J., LEY, R. E., HAMADY, M., FRASER-LIGGETT, C. M., KNIGHT, R. &
1069 GORDON, J. I. 2007. The human microbiome project. *Nature,* 449**,** 804-10.
1070 UNIPROT, C. 2019. UniProt: a worldwide hub of protein knowledge. *Nucleic Acids Res,* 47**,**
1071 D506-D515.
1072 VARSANI, A. & KRUPOVIC, M. 2018. Smacoviridae: a new family of animal-associated single-
1073 stranded DNA viruses. *Arch Virol,* 163**,** 2005-2015.
1074 VICTORIA, J. G., KAPOOR, A., LI, L., BLINKOVA, O., SLIKAS, B., WANG, C., NAEEM, A.,
1075 ZAIDI, S. & DELWART, E. 2009. Metagenomic analyses of viruses in stool samples from
1076 children with acute flaccid paralysis. *J Virol,* 83**,** 4642-51.
1077 WALDOR, M. K. & MEKALANOS, J. J. 1996. Lysogenic conversion by a filamentous phage
1078 encoding cholera toxin. *Science,* 272**,** 1910-4.
1079 WICK, R. R., SCHULTZ, M. B., ZOBEL, J. & HOLT, K. E. 2015. Bandage: interactive
1080 visualization of de novo genome assemblies. *Bioinformatics,* 31**,** 3350-2.
1081 ZERBINI, F. M., BRIDDON, R. W., IDRIS, A., MARTIN, D. P., MORIONES, E., NAVAS-
1082 CASTILLO, J., RIVERA-BUSTAMANTE, R., ROUMAGNAC, P., VARSANI, A. & ICTV
1083 REPORT, C. 2017. ICTV Virus Taxonomy Profile: Geminiviridae. *J Gen Virol,* 98**,** 131-
1084 133.

1085 ZHANG, W., OLSON, N. H., BAKER, T. S., FAULKNER, L., AGBANDJE-MCKENNA, M.,
1086 BOULTON, M. I., DAVIES, J. W. & MCKENNA, R. 2001. Structure of the Maize streak
1087 virus geminate particle. *Virology,* 279**,** 471-7.
1088 ZHAO, L., ROSARIO, K., BREITBART, M. & DUFFY, S. 2019. Eukaryotic Circular Rep-
1089 Encoding Single-Stranded DNA (CRESS DNA) Viruses: Ubiquitous Viruses With Small
1090 Genomes and a Diverse Host Range. *Adv Virus Res,* 103**,** 71-133.
1091 ZIMMERMANN, L., STEPHENS, A., NAM, S. Z., RAU, D., KUBLER, J., LOZAJIC, M., GABLER,
1092 F., SODING, J., LUPAS, A. N. & ALVA, V. 2018. A Completely Reimplemented MPI
1093 Bioinformatics Toolkit with a New HHpred Server at its Core. *J Mol Biol,* 430**,** 2237-2243.
1094

Table S1

Sample Name	haddock1	16minnow	18minnow
Host Animal	Melanogrammus aeglefinus	Pimephales sp.	Pimephales sp.
Tissue/Sample Type	scales, tissue	whole animal	whole animal
Origin	fishmonger	wild	wild
Run	SRR5832142	SRR7122375	SRR7122375
Experiment	SRX3009445	SRX4043871	SRX4043871
BioSample	SAMN07319269	SAMN09074552	SAMN09074552
BioProject	PRJNA393166	PRJNA393166	PRJNA393166
Anelloviridae	0	0	0
Bacilladnaviridae	0	1	0
CRESS virus	55	61	35
Caudovirales	0	2	0
Circoviridae	21	7	3
CrAssphage	0	0	0
Geminiviridae	1	2	0
Genomoviridae	5	7	5
Inoviridae	32	3	0
Microviridae	20	344	111
Myoviridae	0	0	2
Papillomaviridae	2	0	0
Phage	0	3	4
Podoviridae	0	0	0
Siphoviridae	0	0	0
Virus	0	0	0
circular genetic element	52	19	15

pompano1	crucian1	rainbowtrout1	redsnapper1	seabass1	seabass2	seabass3
Trachinotus s	Carassius car	Oncorhynchus	Lutjanus camp	Centropristis s	Centropristis s	Centropristis s
scales, tissue	scales, tissue	scales, tissue	scales, tissue	scales, tissue	scales, tissue	scales, tissue
fishmonger	fishmonger	fishmonger	fishmonger	fishmonger	fishmonger	fishmonger
SRR7122328	SRR7122330	SRR7122364	SRR7122366	SRR7122359	SRR7122360	SRR7109542
SRX4043918	SRX4043916	SRX4043882	SRX4043880	SRX4043887	SRX4043886	SRX4037349
SAMN09074	SAMN09074	SAMN0907453	SAMN0907453	SAMN0907453	SAMN0907453	SAMN0906134
PRJNA39316	PRJNA39316	PRJNA393166	PRJNA393166	PRJNA393166	PRJNA393166	PRJNA393166
0	0	0	0	0	0	0
0	0	0	2	0	0	0
2	32	22	81	19	6	5
0	0	0	0	0	0	0
1	12	20	104	13	5	5
0	0	0	0	0	0	0
0	0	0	1	1	0	0
0	0	3	0	0	0	0
0	0	5	1	3	0	0
0	10	6	42	0	1	0
0	0	0	0	0	0	0
0	0	1	1	0	0	0
0	1	1	3	0	0	0
0	0	0	0	0	0	0
0	0	0	1	0	0	0
0	0	0	6	0	0	0
1	1	19	271	20	5	2

seabass4	seabass_ms2	worm1	squid1	abalone1	crab1
Centropristis s	Centropristis s	Rhabditidae s	unidentified s	Haliotis sp.	Callinectes sa
scales, tissue	scales, tissue	whole animal	tissue	whole animal	prepared me
fishmonger	fishmonger	wild	supermarket	supermarket	supermarket
SRR7122361	SRR7501340	SRR7122374	SRR7122358	SRR7122363	SRR7122357
SRX4043885	SRX4370701	SRX4043872	SRX4043888	SRX4043883	SRX4043889
SAMN0907453	SAMN0963426	SAMN09074	SAMN09074	SAMN09074535	SAMN09074
PRJNA393166	PRJNA393166	PRJNA39316	PRJNA39316	PRJNA393166	PRJNA39316
0	0	0	0	0	0
0	0	0	0	0	0
4	98	1	1	84	9
0	0	0	0	0	0
2	50	0	0	30	3
0	0	0	0	0	0
0	2	0	0	0	0
0	0	0	0	6	0
2	2	0	1	2	0
0	6	2	0	6	0
0	1	0	0	0	0
0	0	0	0	0	0
0	0	1	0	0	0
0	1	3	0	0	0
0	2	6	0	0	0
0	0	0	0	0	0
11	77	0	0	71	2

fly1	axolotl1	axolotl_blastema1	turkey	10mus
Drosophila sp.	Ambystoma mexicanum	Ambystoma mexicanum	Meleagris gal	Mus musculus
whole animals	skin swab	blastema	ground meat	skin tissue
wild	laboratory animal	laboratory animal	supermarket	laboratory animal
SRR7122373	SRR7122381	SRR7122338	SRR7122322	SRR7122376
SRX4043873	SRX4043865	SRX4043908	SRX4043924	SRX4043870
SAMN09074550	SAMN09074558	SAMN09074560	SAMN09074	SAMN09074553
PRJNA393166	PRJNA393166	PRJNA393166	PRJNA393166	PRJNA393166
0	0	0	0	0
0	0	0	0	0
0	1	1	2	3
1	0	0	0	0
1	0	0	2	0
0	0	0	0	2
0	0	0	0	0
1	0	0	2	1
0	0	1	1	4
1	0	0	2	12
3	0	0	0	0
0	0	0	0	0
0	0	0	0	0
1	1	0	0	3
5	0	0	0	2
0	0	0	0	0
0	1	2	4	3

mice_vaginal	apo1	apo2	raccoon_spleen_ga11
Mus musculus	Apodemus sylvaticus	Apodemus sylvaticus	Procyon lotor
vaginal swabs	skin tissue	skin tissue	spleen tissue
wild	wild	wild	wild (UC-Davis)
SRR7122365	SRR7122347	SRR7122346	SRR7122354
SRX4043881	SRX4043899	SRX4043900	SRX4043892
SAMN09074573	SAMN09074600	SAMN09074601	SAMN09074580
PRJNA393166	PRJNA393166	PRJNA393166	PRJNA393166
0	0	0	2
0	0	0	0
1	7	3	0
0	0	0	0
1	1	2	0
0	0	0	0
0	0	1	0
0	16	3	0
1	0	0	0
3	1	0	0
0	1	0	0
0	0	0	0
0	0	0	0
0	0	0	0
0	1	0	0
0	0	0	0
0	6	2	0

raccoon_spleen_ga014	raccoonskin1	beef_bd3	beef_bd4	bison1	bison2
Procyon lotor	Procyon lotor	Bos taurus	Bos taurus	Bison bison	Bison bison
spleen tissue	skin tissue	ground meat	ground meat	ground meat	ground meat
wild (UC-Davis)	wild (UC-Davis)	supermarket	supermarket	supermarket	supermarket
SRR7122350	SRR7122367	SRR7122336	SRR7122333	SRR7122319	SRR7122320
SRX4043896	SRX4043879	SRX4043910	SRX4043913	SRX4043927	SRX4043926
SAMN09074579	SAMN09074538	SAMN09074	SAMN09074	SAMN09074	SAMN09074
PRJNA393166	PRJNA393166	PRJNA39316	PRJNA39316	PRJNA39316	PRJNA39316
13	0	0	0	0	0
0	0	0	0	0	0
0	9	4	1	2	3
0	0	0	0	0	0
0	6	3	1	0	1
0	0	0	0	0	0
0	0	0	0	0	0
0	2	0	1	0	1
0	0	0	0	1	0
0	0	2	0	1	0
0	0	0	0	0	0
0	0	0	0	0	0
0	0	0	0	0	0
0	0	0	0	0	0
0	0	0	0	0	0
0	0	0	0	0	0
0	6	9	0	6	0

lamb1	pig1	macstool_D2CW	macstool_cl86	macstool_dcvf
Ovis aries	Sus scrofa	Macaca mulatta	Macaca mulatta	Macaca mulatta
ground meat	ground meat	feces	feces	feces
supermarket	supermarket	laboratory animal	laboratory animal	laboratory animal
SRR7122321	SRR7122327	SRR7122355	SRR7122337	SRR7122353
SRX4043925	SRX4043919	SRX4043891	SRX4043909	SRX4043893
SAMN09074	SAMN09074	SAMN09074562	SAMN09074561	SAMN09074563
PRJNA39316	PRJNA39316	PRJNA393166	PRJNA393166	PRJNA393166
0	13	0	0	0
0	0	0	0	0
3	1	0	1	0
0	0	0	0	0
1	0	0	1	1
0	0	0	0	0
0	0	0	0	0
2	2	0	0	1
0	0	1	1	2
1	0	13	13	27
0	0	0	0	0
0	0	0	0	0
0	0	0	0	0
0	0	0	0	0
0	0	0	0	0
0	0	0	0	0
2	0	0	0	0

macstool_de1a	macstool_de2c	W01_blood	W07_blood	ms19_W08
Macaca mulatta	Macaca mulatta	Homo sapiens	Homo sapiens	Homo sapiens
feces	feces	blood	blood	blood
laboratory animal	laboratory animal	clinical (NIH CCR)	clinical (NIH CCR)	clinical (NIH CCR)
SRR7122342	SRR7122341	SRR6442920	SRR6442879	SRR6442889
SRX4043904	SRX4043905	SRX3534153	SRX3534194	SRX3534184
SAMN09074564	SAMN09074565	SAMN08296098	SAMN08296113	SAMN08296116
PRJNA393166	PRJNA393166	PRJNA396064	PRJNA396064	PRJNA396064
0	0	4	2	44
0	0	0	0	0
2	3	0	0	0
0	0	0	0	0
1	2	0	0	0
0	0	0	0	0
0	0	0	0	0
0	0	0	0	0
2	5	0	0	0
19	27	0	0	0
0	0	0	0	0
0	0	0	0	0
0	1	0	0	0
0	1	0	0	0
1	0	0	0	0
0	0	0	0	0
2	0	0	0	0

ms19_W18	ms19_W27	brain1	brain2	brain3	brain4
Homo sapiens	Homo sapiens	Homo sapiens	Homo sapien	Homo sapien	Homo sapien
blood	blood	brain tissue, Non-A	brain tissue, I	brain tissue, A	brain tissue, A
clinical (NIH CCR)	clinical (NIH CCR)	clinical (Johns Hop	clinical (Johns	clinical (NIH A	clinical (NIH A
SRR6442898	SRR6442973	SRR7122324	SRR7122344	SRR7122349	SRR7122313
SRX3534175	SRX3534100	SRX4043922	SRX4043902	SRX4043897	SRX4043933
SAMN08296125	SAMN08296159	SAMN09074582	SAMN090745	SAMN090745	SAMN090745
PRJNA396064	PRJNA396064	PRJNA393166	PRJNA393166	PRJNA393166	PRJNA393166
24	68	0	0	0	0
0	0	0	0	0	0
0	0	0	0	0	0
0	0	0	0	0	0
0	0	0	0	0	0
0	0	0	0	0	0
0	0	0	0	0	0
0	0	0	0	0	0
0	0	0	0	0	0
0	0	0	0	0	0
0	0	0	0	0	0
0	0	0	0	0	0
0	0	0	0	0	0
0	0	0	0	0	0
0	0	0	0	0	0
0	0	0	0	0	0
0	0	0	0	0	0
0	0	0	0	0	0

brain5	brain6	brain7	brain8	brain9	brain10	brain11
Homo sapien	Homo sapien	Homo sapien	Homo sapien	Homo sapien	Homo sapien	Homo sapien
brain tissue, A	brain tissue, A	brain tissue, I	brain tissue, I	brain tissue, A	brain tissue, I	brain tissue, A
clinical (NIH A	clinical (NIH A	clinical (Johns	clinical (Johns	clinical (NIH A	clinical (Johns	clinical (NIH A
SRR7122314	SRR7122316	SRR7122317	SRR7122318	SRR7122315	SRR7122343	SRR7122356
SRX4043932	SRX4043930	SRX4043929	SRX4043928	SRX4043931	SRX4043903	SRX4043890
SAMN09074	SAMN09074	SAMN09074	SAMN09074	SAMN09074	SAMN09074	SAMN09074
PRJNA39316	PRJNA39316	PRJNA39316	PRJNA39316	PRJNA39316	PRJNA39316	PRJNA39316
0	0	0	0	0	0	0
0	0	0	0	0	0	0
0	0	0	0	0	0	0
0	0	0	0	0	0	0
0	0	0	0	0	0	0
0	0	0	0	0	0	0
0	0	0	0	0	0	0
0	0	0	0	0	0	0
0	0	0	0	0	0	0
0	0	0	0	0	0	0
0	0	0	0	0	0	0
0	0	0	0	0	0	0
0	0	0	0	0	0	0
0	0	0	0	0	0	0
0	0	0	0	0	0	0
0	0	0	0	0	0	0
0	0	0	0	0	0	0
0	0	0	0	0	0	0

brain12 TOTAL Taxon
Homo sapiens
brain tissue, Non-Alzheimer's Dementia, CERAD=0, BRAAK=2
clinical (Johns Hopkins ADRC)
SRR7122345
SRX4043901
SAMN09074585
PRJNA393166

0	170	Anelloviridae
0	3	Bacilladnaviridae
0	562	CRESS virus
0	3	Caudovirales
0	300	Circoviridae
0	2	CrAssphage
0	8	Geminiviridae
0	58	Genomoviridae
0	70	Inoviridae
0	670	Microviridae
0	7	Myoviridae
0	4	Papillomaviridae
0	14	Phage
0	10	Podoviridae
0	18	Siphoviridae
0	6	Virus
0	609	circular genetic element
	2514	

Table S2

Microviridae sp. isolate ctgd198
MH552479

Illumina Library	SRR #	Illumina sequencing run #	Contig Coverage Depth
10mus	SRR7122376	18	97.2
bison1	SRR7122319	4	50.5
haddock1	SRR5832142	12	18.7
rainbowtrout1	SRR7122364	14	37.9

Inoviridae sp. isolate ctda6
MH552488

Illumina Library	SRR #	Illumina sequencing run #	Contig Coverage Depth
abalone1	SRR7122363	12	21.8
W01_blood	SRR6442920	19	62.4
ms19_W08	SRR6442889	19	3.5
ms19_W18	SRR6442898	19	2.5
ms19_W27	SRR6442973	19	3.4

CRESS virus sp. isolate ctbd281
MH617267

Illumina Library	SRR #	Illumina sequencing run #	Contig Coverage Depth
abalone1	SRR7122363	12	8.1
bison2	SRR7122320	4	84.9
haddock1	SRR5832142	12	73.9
squid1	SRR7122358	12	4.6

CRESS virus sp. isolate cthf761
MH552486

Illumina Library	SRR #	Illumina sequencing run #	Contig Coverage Depth
10mus	SRR7122376	18	65.1
apo1	SRR7122347	18	115.7
redsnapper1	SRR7122366	3	31.4

Circular genetic element sp. isolate ctbf001
MH648779

Illumina Library	SRR #	Illumina sequencing run #	Contig Coverage Depth
beef_bd3	SRR7122336	3	28.7
raccoonskin1	SRR7122367	8	10.1

Circular genetic element sp. isolate ctbi451

MK012536

Illumina Library	SRR #	Illumina sequencing run #	Contig Coverage Depth
10mus	SRR7122376	18	65.1
apo1	SRR7122347	18	115.7
beef_bd3	SRR7122336	3	11.1
bison1	SRR7122319	4	11.3
bison2	SRR7122320	4	5
lamb1	SRR7122321	4	9.4
haddock1	SRR5832142	12	8.9
redsnapper1	SRR7122366	3	31.4
turkey	SRR7122322	4	6